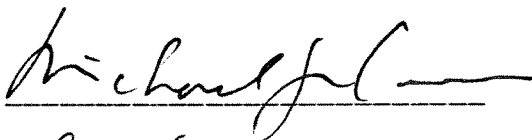


INVERSE MODELING OF ALKALINE LAVAS FROM GUAYACAN,
COSTA RICA

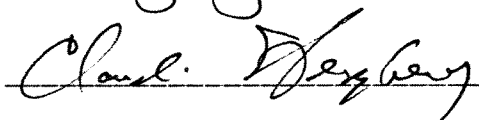
BY CRISTINA M. STACK

A thesis submitted to the
Graduate School-New Brunswick
Rutgers, The State University of New Jersey
in partial fulfillment of the requirements
for the degree of
Master of Science
Graduate Program in Geological Sciences

Written under the direction of
Michael J. Carr and Mark D. Feigenson
and approved by







New Brunswick, New Jersey

October, 1991

ABSTRACT OF THE THESIS
INVERSE MODELING OF ALKALINE LAVAS FROM GUAYACAN,
COSTA RICA

By Cristina M. Stack

Thesis Advisors: Michael J. Carr and Mark D. Feigenson

A suite of subalkaline to alkaline lavas of Pliocene age (4.6 My) from central Costa Rica provides an ideal rare earth element data set for inverse modeling to determine mantle source characteristics. Samples were collected from a drill core that penetrated the entire Formación Alkalina de Guayacán at a dam site on the Rio Pacuare. Twenty-four of the 27 lava flows in the complete 256 meter thick section were sampled.

These alkaline rocks have an MgO range of 7.1 to 12.4 wt. %. Isotopes of Sr and Nd were measured on 5 samples that span the section and yield values analytically indistinguishable from the mean values of 0.703570 and 0.512965, respectively. Lanthanum varies in the lavas between 17 and 74 ppm and the lavas are all light REE enriched, with La/Sm and La/Yb values ranging from 3 to 7 and 11 to 35, respectively.

The constant isotopic values imply a homogeneous source for use in inverse modeling. The method used follows Hofmann and Feigenson (1983) and assumes batch melting. Both uncorrected data and data corrected for small amounts of olivine and clinopyroxene fractionation were used as models. Results for the two models show that the source must be moderately light REE enriched, with La/Sm and La/Yb ratios that range from 2 to 4 and 2 to 10, respectively. The degrees of melting of the source range

from <0.5% to 4% based on an assumed source La concentration of 0.66 ppm (Carr et al., 1990). Calculated initial source partition coefficients suggest that the clinopyroxene to garnet ratios range between 1:5 and 4.3:1, with an average ratio of approximately 1:1.

The source concentration patterns calculated using a Rayleigh melting and a "blended variable batch melting" model are similar in shape to the light REE enriched pattern calculated by the batch melting based inverse modeling. Forward modeling of these source patterns provided measured REE patterns with an acceptable match using the "blended variable batch melting" model, but not the Rayleigh melting model. Further work needs to be done in the area of mantle melt modeling, and from the results seen here, the "variable" melting model should be among those investigated.

ACKNOWLEDGEMENTS

I would especially like to thank ICE for their hospitality and for the opportunity to collect samples. I would also like to thank José Francisco Cervantes Loiaza, Alan Lopez, and Ileana Boschini for all of their help while in Costa Rica. Of course this paper would not have been possible without my advisors Michael J. Carr and Mark D. Feigenson, or the NSF Grant EAR-9005053.

TABLE OF CONTENTS

	Page
ABSTRACT	ii
ACKNOWLEDGEMENTS	iv
TABLE OF CONTENTS	v
LIST OF FIGURES	vii
LIST OF TABLES	viii
I. INTRODUCTION	1
II. GEOLOGIC SETTING	1
III. DATA	3
A. Sampling	3
B. Analytical techniques	8
C. Petrography	8
D. Rock identification	10
E. Sr and Nd isotopes	10
IV. INTERPRETATION OF RESULTS	15
A. Inverse modeling	15
(1) Fractional crystallization correction	16
(2) Process identification and source homogeneity testing	17
(3) Calculation of relative concentrations in the initial source	21
(4) Estimation of relative source mineral abundances	26
B. Rayleigh melting	28
C. Blended variable batch melting	32
V. SUMMARY AND CONCLUSIONS	34
APPENDIX I - Whole Rock Analyses	38

APPENDIX II - Whole rock data corrected for fractional crystallization	46
APPENDIX III - Procedure for separating REEs	49
REFERENCES	50

FIGURES

Figures	Page
1. Tectonic setting of Costa Rica	2
2. Location of Central American volcanoes	4
3. Location of drill cores along the Pacuare River	5
4. Stratigraphic sections for drill cores	6
5. Histogram of modal % phenocrysts	9
6. Rock identification diagram	11
7A,B. Rare earth element profiles. A. Uncorrected data B. Corrected data	12
8. Mixing model for incompatible element ratios	13
9. Mixing model for isotopic element ratios	14
10A,B. Process identification diagrams. A. Uncorrected data B. Corrected data	18,19
11. Lanthanum-magnesia variation diagram	22
12A,B. Relative source concentrations and bulk partition coefficients. A. Uncorrected data B. Corrected data	24,25
13. REE patterns for spinel lherzolite.	27
14. REE patterns for fractional melting model. cpx:gt = 4:1.	30
15. REE patterns for fractional melting model. cpx:gt = 10:1.	31
16. REE patterns for blended variable batch melting model. cpx:gt = 10:1.	35

TABLES

1.	Modal analyses of selected thin sections	7
2.	Sr and Nd isotopic data	15
3A,B.	Slopes and intercepts from the process identification diagrams. A. Uncorrected data B. Corrected data	20
4.	Partition coefficients	23

I. INTRODUCTION

The investigation presented here uses inverse modeling to calculate initial concentrations and source mineralogy from the variations in rare earth elements (REE) in a suite of lavas. The model used assumes batch melting and is that of Hofmann and Feigenson (1983), simplified from Minster and Allegre (1978). The samples collected are Pliocene in age (4.6 My) (Tournon, 1984) and are from a complete section of lavas near Siquirres, Costa Rica. Tournon (1973) was first to comment on the alkaline nature of these lavas which were initially called Formación Teschenita de Guayacán, a name proposed by Kussmaul (1987). Cervantes and Soto (1988), however, found the formation to be of greater extent and amplified the formal name to Formación Alcalina (Teschenita y basalto) de Guayacán. This Guayacán suite of subalkaline to alkaline lavas provides an ideal REE data set because, as shown below, it meets the model's criteria of being cogenetic, relatively unfractionated, and related to one another by different degrees of partial melting. A Rayleigh melting model and a more complicated, "blended variable batch melting" model are used to calculate REE source concentrations and in forward modeling. They are then compared to each other and to the batch melting of the inverse modeling.

II. GEOLOGIC SETTING

Figure 1 illustrates the tectonic setting of Costa Rica where the Cocos plate is subducting beneath the Caribbean plate. The underthrusting of the Cocos plate is thought to be the cause of the Quaternary volcanic front of Central America (Molnar and Sykes,

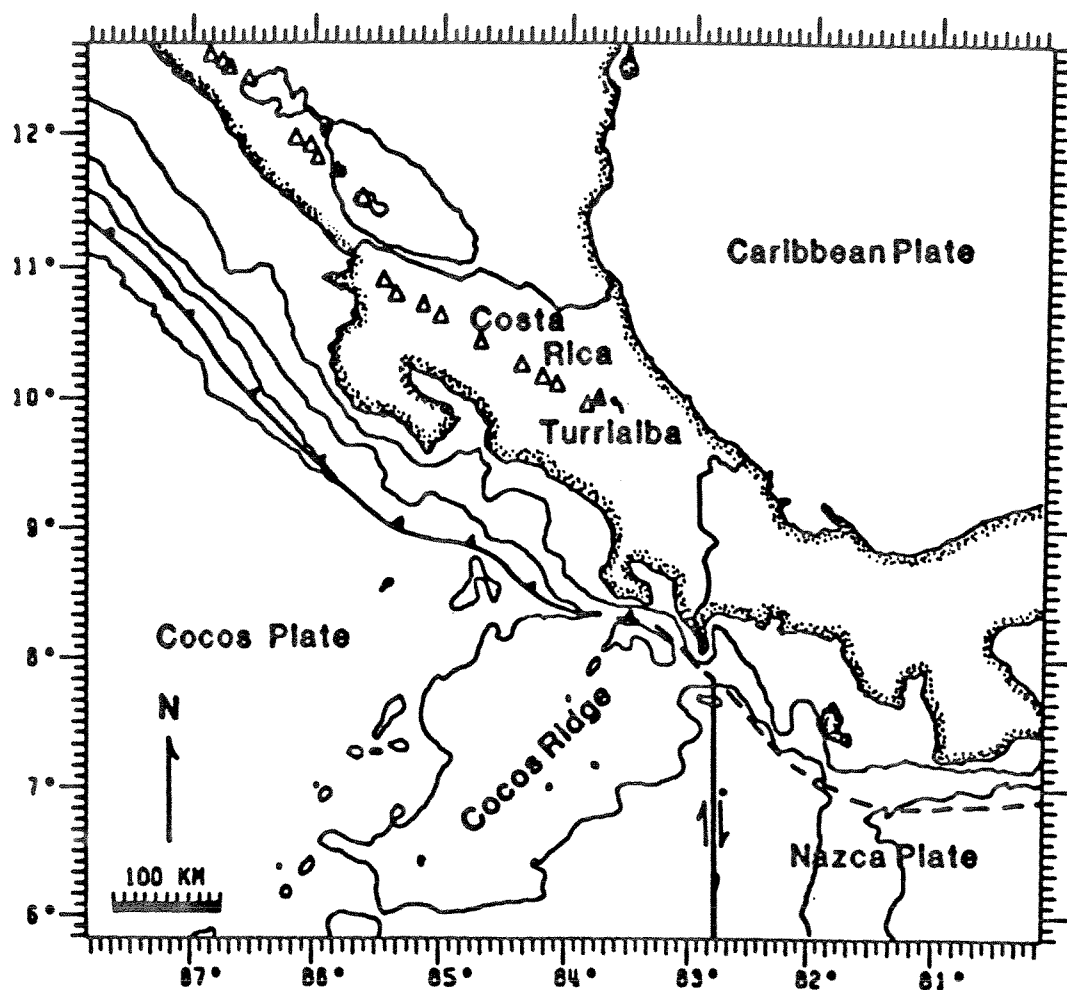


Fig. 1. Tectonic setting of Costa Rica (after Reagan and Gill, 1989).

1969). This volcanic front consists of 40 volcanic centers with basalt, andesite, and dacite cones and stretches from the Mexico-Guatemala border to central Costa Rica (Fig. 2). There is a 200 km gap between the end of the Central American volcanic front and the next volcano, located farther southeast in Panama (Carr and Stoiber, 1990). The basement below Costa Rica is Mesozoic oceanic crust whereas the basement for the remainder of the volcanic front (Guatemala, El Salvador and Nicaragua) is Paleozoic metamorphic rocks (Weyl, 1980). In Costa Rica, cones behind the volcanic front are mainly alkaline basalts. Samples in this study were collected from lavas approximately 30 km east of Turrialba, the southeasternmost volcano in the Central American volcanic front (Fig. 1).

III. DATA

A. Sampling

Thirty-nine samples were collected from two cores 4.7 cm in diameter, drilled by the Costa Rican electric company (Instituto Costarricense de Electricidad) (Fig 3). Core PSQ-21 penetrated the entire 256 m thick section and core PSQ-24 the upper 144 m of Formación Alkalina de Guayacán at a dam site on the Rio Pacuare. Twenty-five samples were taken from 24 of the 29 lava flows in core PSQ-21 (Fig 4). Fourteen samples were collected from 20 lava flows in core PSQ-24. The lava flows range in thickness from 1.2 m to 21.3 m. Three samples were collected along roads between the towns of Siquirres and Guayacán. A sample of teschenite was also collected from the area.

Lavas were sampled in the freshest areas of flow interiors

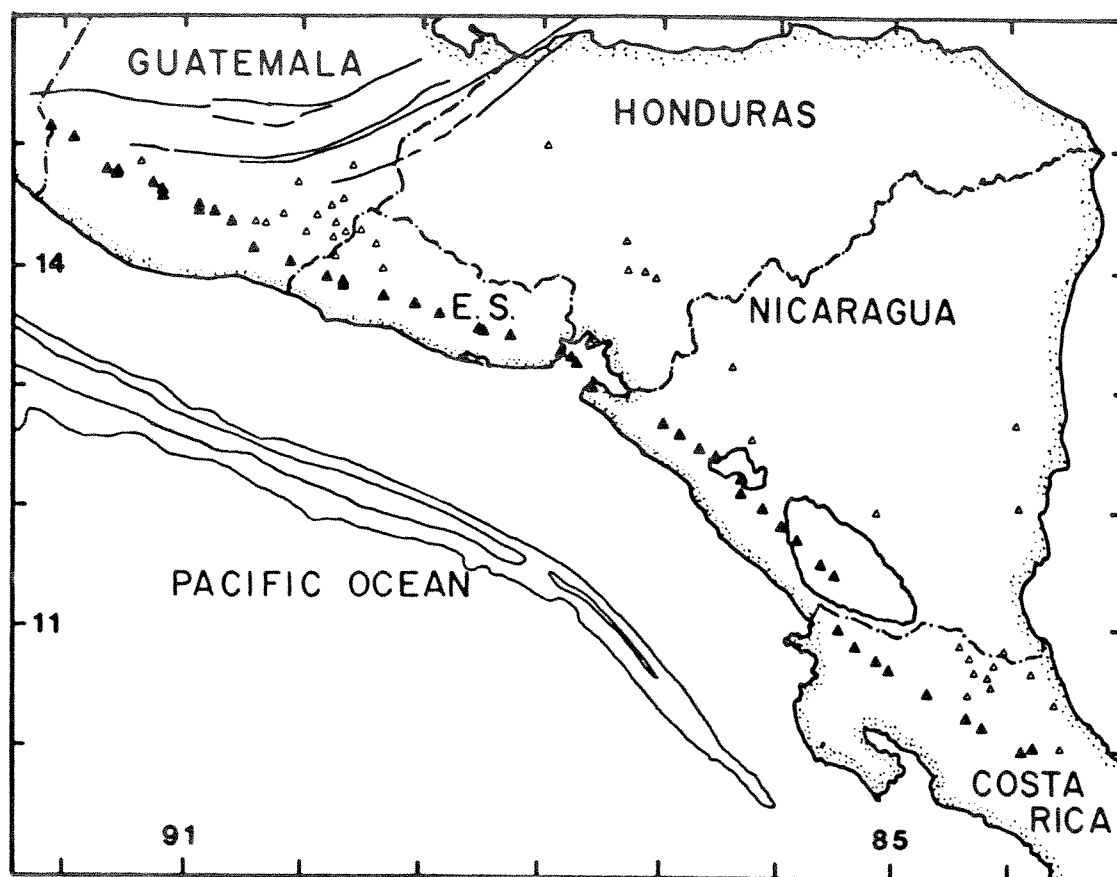
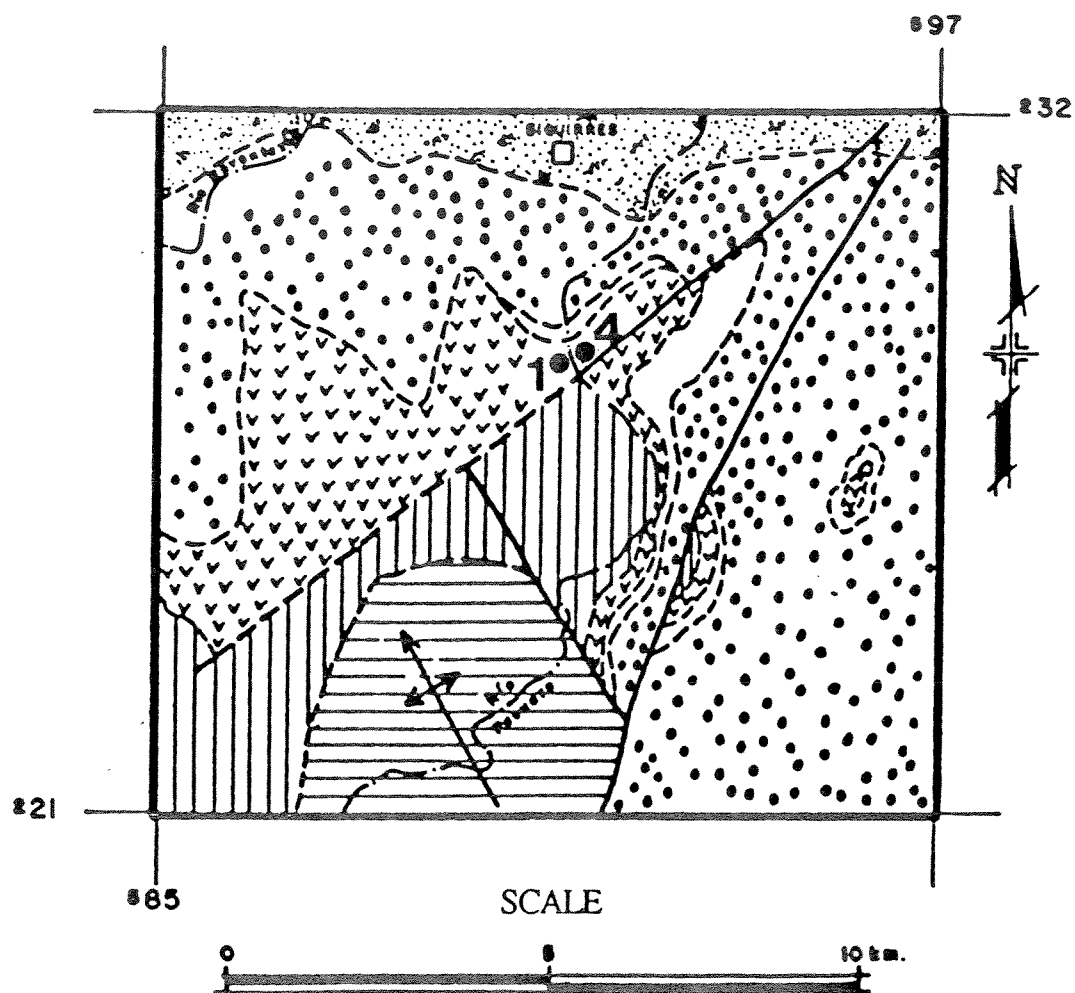


Fig. 2. Locations of Central American volcanoes. Solid triangles = volcanoes on the volcanic front, open triangles = volcanoes behind the front. E.S. is El Salvador. Contours mark the position of Middle America Trench.



LEGEND

- RECENT ALLUVIAL DEPOSITS
- SURETKA FM (PLIOCENE-PLEISTOCENE)
- ALKALINE LAVAS (PLIOCENE)
- RIO BANANO FM (UPPER MIOCENE-PLIOCENE)
- USCARI FM (UPPER OLIGOCENE-UPPER MIOCENE)
- TUIS FM (MIDDLE EOCENE)
- FAULT
- FOLD
- LITHOLOGIC CONTACT

Fig. 3. Locations of drill cores along the Pacuare River (after Cervantes and Soto, 1988). 1 = PSQ-21; 4 = PSQ-24.

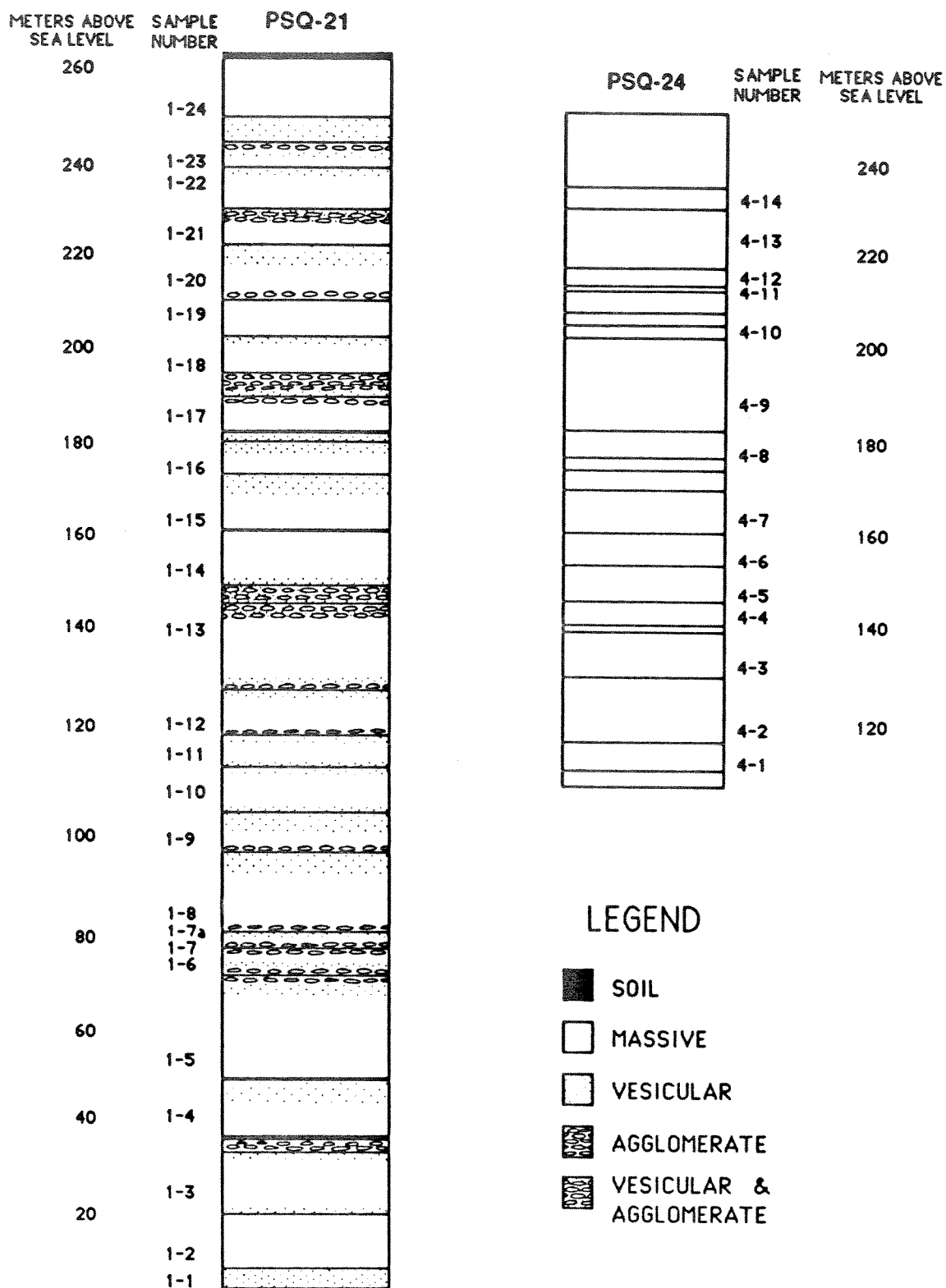


Fig. 4. Stratigraphic sections for drill cores PSQ-21 and PSQ-24. Lithologic units only shown for PSQ-21.

with as little vesiculation or alteration as possible. When samples were split and crushed in the laboratory, only the least altered pieces were chosen to be powdered and analyzed. Some samples, however, still showed the affects of alteration as is seen in lower totals from major and trace element analyses (Appendix I).

Eighteen samples spanning the two sections were chosen for rare earth element analysis from those samples that had totals greater than 95% after major and trace element analyses (Appendix I).

Whole rock analyses corrected for fractional crystallization are included as Appendix II.

Thin sections were made for most of the samples analyzed for rare earth elements. These helped in determining the phenocrysts present, the freshest samples, and those appropriate for electron microprobe analysis. A categorization of some of the samples into degrees of alteration (low, moderate, high) is found in Table 1.

Table 1. Modal analyses of selected thin sections

Sample	% ol	% cpx	Total %	Degree of Alteration*
1-3	11.2	0.0	11.2	moderate
1-4	11.5	1.7	13.2	low
1-5	9.5	0.0	9.5	high
1-12	10.0	0.0	10.0	moderate
1-14	8.7	0.0	8.7	low
1-18	9.6	0.9	10.5	low
1-21	8.8	0.0	8.8	moderate
1-24	4.8	0.0	4.8	low
GU-2	9.4	0.3	9.7	low

*Degrees of alteration given are relative to each other.

B. Analytical Techniques

All major, trace and rare earth element measurements were made by dc-plasma atomic emission spectroscopy (DCP-AES) at Rutgers University following Feigenson and Carr (1985). The procedure for REE separation is in Appendix III. Our in-house standard, IZ, as well as the USGS standards BCR, BHVO, AGV, GSP, W1, G2 and JB1A were run with the unknowns. Mineral compositions were determined from thin sections using the electron microprobe at Rutgers University.

Sr and Nd isotopic ratios were measured a VG Sector mass spectrometer at Rutgers University. Sr isotopic ratios are normalized to $^{86}\text{Sr}/^{88}\text{Sr}$ of 0.1194 and Nd isotopic ratios are normalized to $^{146}\text{Nd}/^{144}\text{Nd}$ of 0.7219. NBS SRM 987 is measured at $^{87}\text{Sr}/^{86}\text{Sr} = 0.710251$ and La Jolla Std Nd is measured at $^{143}\text{Nd}/^{144}\text{Nd} = 0.511852$. Internal precision is reported in Table 2; external precision is given in the footnote to Table 2. Both Sr and Nd isotopic ratios are reported as measured in Table 2.

C. Petrography

The samples collected are microcrystalline with phenocrysts of olivine (Fo_{77-89}), 5.0-0.1 mm in length. Some samples contain phenocrysts of clinopyroxene ($\text{Wo}_{48-52}\text{En}_{33-43}\text{Fs}_{9-15}$), 1.0-0.1 mm in length. Results of modal analysis of 9 samples (Table 1) indicate the range in olivine and clinopyroxene phenocrysts are 4-12% and 0-2%, respectively. The distribution of phenocrysts is shown in a histogram in Figure 5.

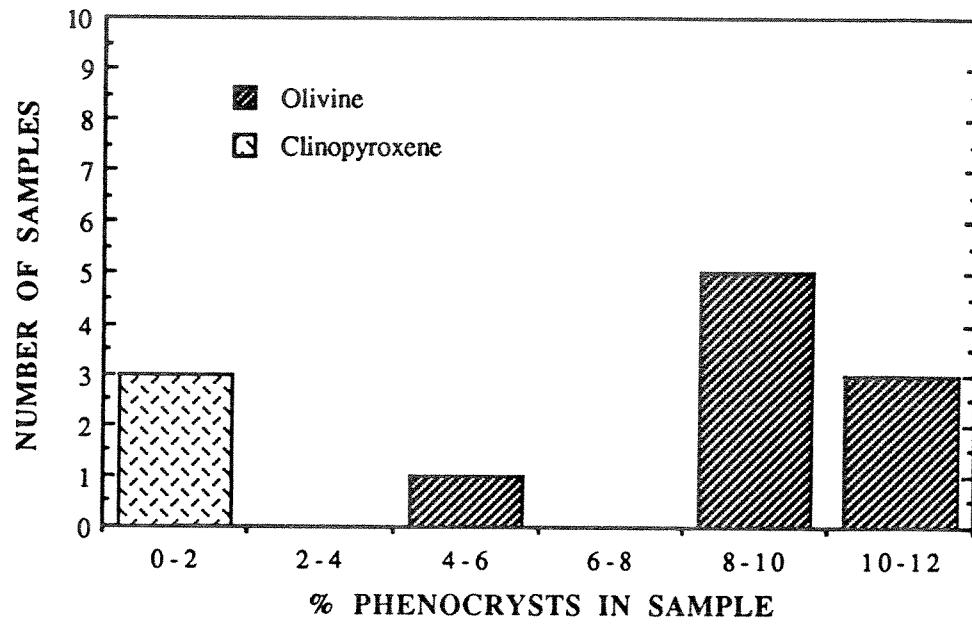


Fig. 5. Histogram of modal % olivine and clinopyroxene phenocrysts from 9 thin sections.

D. Rock Identification

Figure 6 is a plot of alkalis vs wt.% SiO₂. It demonstrates the predominant alkaline nature of these basaltic lavas. The lavas have an MgO range of 7.1 to 12.4 wt.% and an SiO₂ range of 41.1 to 48.9 wt.%. Spider diagrams of both uncorrected and corrected REE data (Fig. 7A and 7B) show how the lavas are light REE enriched. Lanthanum varies between 17 and 74 ppm, and La/Sm and La/Yb values range from 3 to 7 and 11 to 35, respectively.

Figure 8 illustrates a mixing model by Carr et al. (1990) that roughly estimates degrees of melting. The source concentration of La in the mixing model is assumed to be 0.66 ppm. The Guayacán data plotted on this model suggests that it is derived from small degrees of melting (<0.5%) of enriched mantle (EM) to 3 or 4% melting of a mixture of EM and small amounts of modified mantle (MM) or fluid released from the subducted slab. The data only fit the mixing model approximately, possibly because the smallest degree melts are less than 0.5% and the knowledge of the composition of EM is not definite. The model would also change with the use of different partition coefficients; however, it still gives a general idea of the degrees of melting and mantle compositions of the samples.

E. Sr and Nd Isotopes

Isotopes of Sr and Nd were measured on 5 samples (Table 2) taken from across the section and yield values analytically indistinguishable from the mean values of 0.703570 and 0.512965, respectively. The Sr and Nd isotopic data are plotted in Fig. 9 along with the field of data from the volcanic front of Central

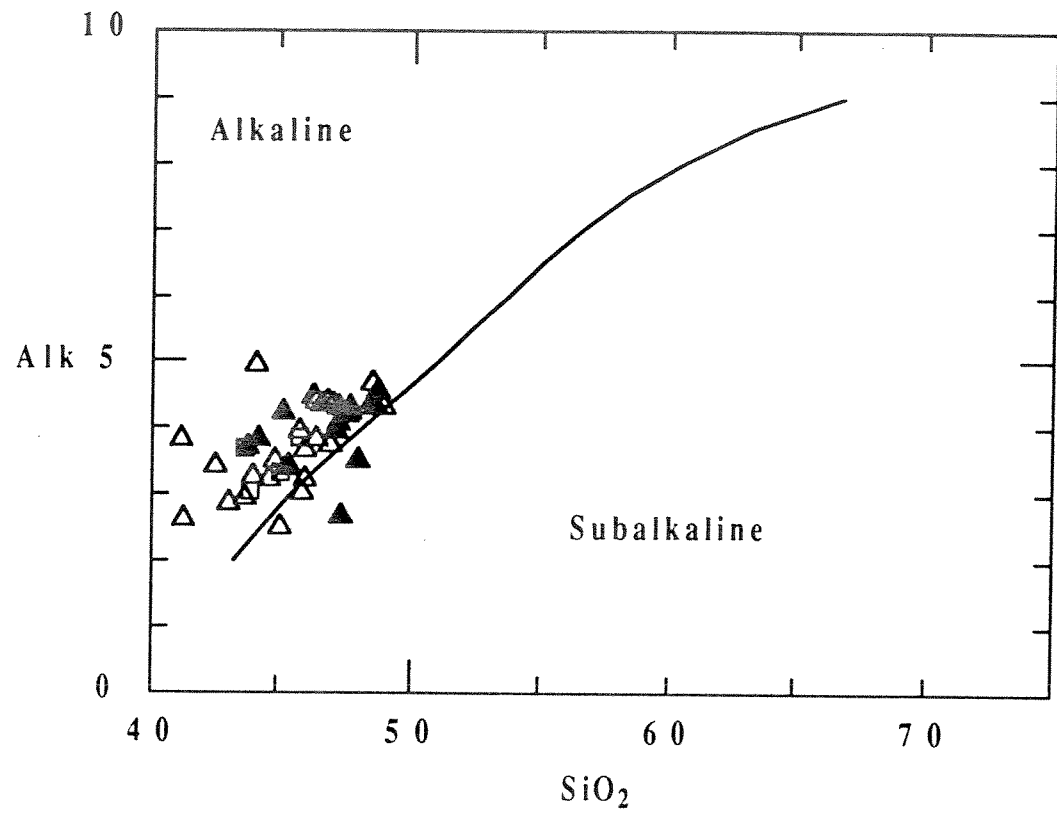


Fig. 6. Rock identification diagram. Open triangles = PSQ-21, filled triangles = PSQ-24, open squares = samples from along the road.

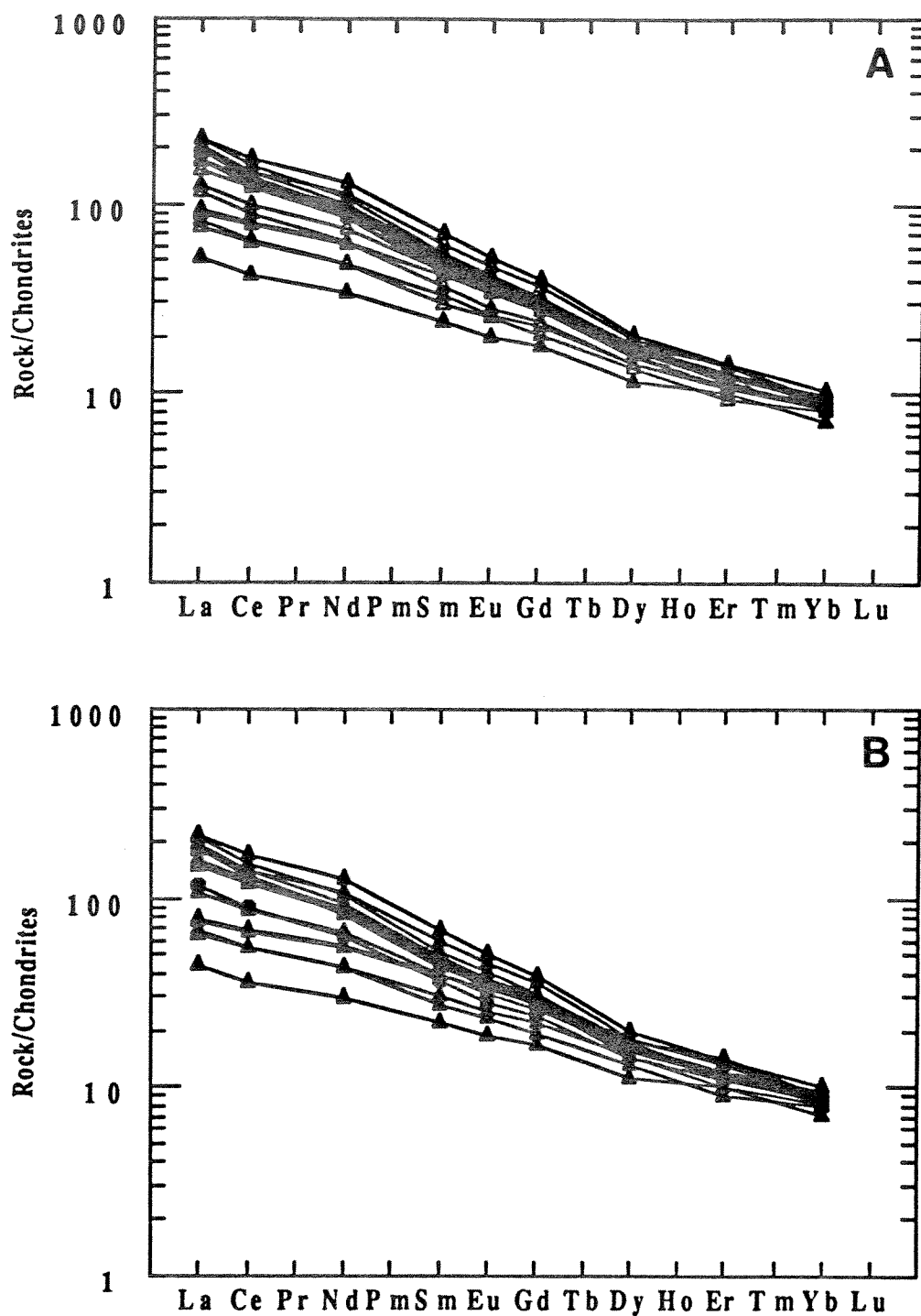


Fig. 7A, B. Rare earth element profiles showing a large range in LREE concentrations and a small range in HREE. A. Uncorrected data. B. Corrected data.

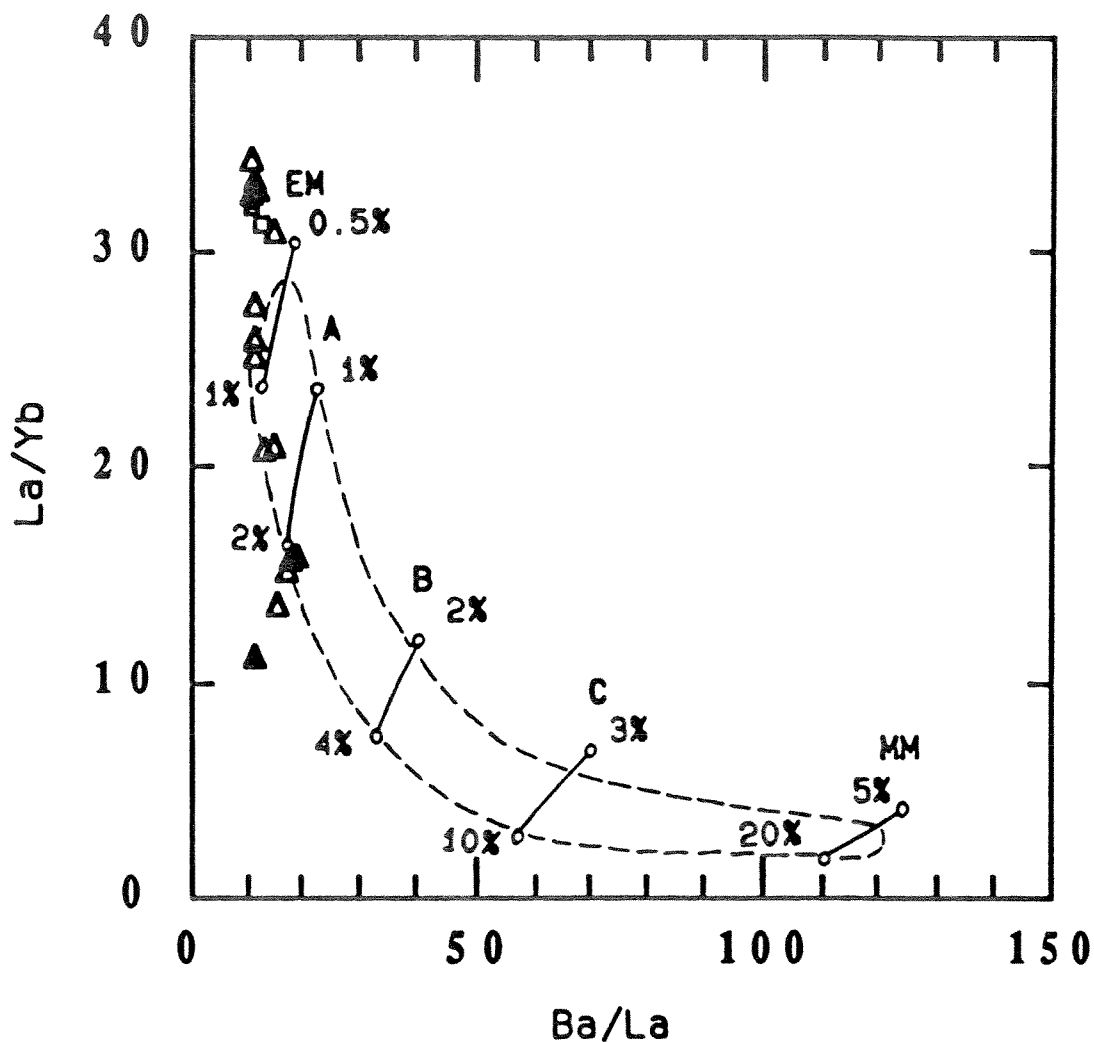


Fig. 8. Mixing model for incompatible element ratios. DM, depleted mantle; EM, "enriched" mantle; A, B, C and MM (modified mantle) are metasomatized sources. New data is plotted with the field of volcanic front samples and magnesian and alkaline lavas of central Costa Rica. Lines marked EM, A, B, C, and MM show expected incompatible element ratios for batch partial-melting of these mantle sources. Melt percentages are marked, (after Carr et. al, 1990).

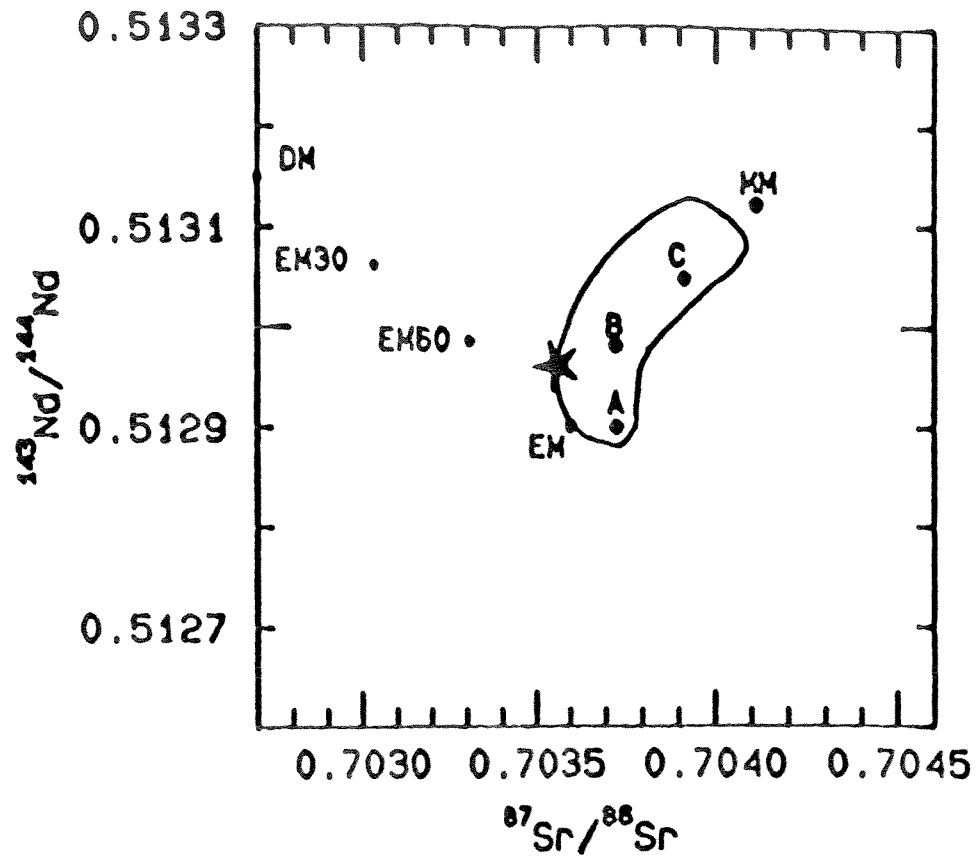


Fig. 9. Mixing model for isotopic element ratios. DM, depleted mantle; EM, "enriched" mantle; A, B, C and MM (modified mantle) are metasomatized sources. Clean mantle mixtures of DM and EM are modified by sediment-derived fluid. Star = average isotope ratios, Bubble = area where the main trend of Central American data plot.

America. The Guayacán data appears to be a low Sr end-member. The nearly identical isotopic values of these rocks suggests a homogeneous source, making this suite suitable for inversion.

Table 2. Sr and Nd isotopic data

Sample	Sr	Nd
1 - 5	0.703569 \pm 12	0.512960 \pm 3
1 - 14	0.703579 \pm 40	0.512969 \pm 3
1 - 17	0.703539 \pm 26	0.512963 \pm 4
1 - 18	0.703591 \pm 30	0.512964 \pm 4
1 - 21	0.703560 \pm 13	0.512971 \pm 3
1 - 24	0.703579 \pm 28	-----

----- = no data. Average Sr = 0.703570 \pm 18 and Nd = 0.512965 \pm 5. Error on average is \pm 1 standard deviation of mean.

IV. INTERPRETATION OF RESULTS

A. Inverse Modeling

Inverse modeling was initiated in 1968 with a paper by Gast. In this paper, Gast used Henry's Law and the Nernst Distribution Law to quantify factors governing trace element concentrations. Soon afterward, Shaw (1970) expanded on Gast's equations. Shaw's equations were then used by Minster and Allegre in 1978 for their inverse modeling.

The Hofmann and Feigenson (1983) model used here assumes batch melting and is a mathematically simplified version of the Minster and Allegre (1978) geochemical inversion technique. To use this model, samples must be relatively unfractionated and related by a homogeneous source and different degrees of partial melting. Variations in REE concentrations of the samples are systematically modelled to calculate initial concentrations and source mineralogy. Rare earth elements are

used as opposed to major or other trace elements because their geochemical behavior varies regularly as a function of atomic number, and because they are more resistant to mobilization during alteration.

Four steps, slightly modified from Hofmann and Feigenson (1983), were followed for the inverse modeling process and are described in detail below. The steps are (1) fractional crystallization correction, (2) process identification and source homogeneity testing, (3) calculation of relative concentrations in the initial source, and (4) estimation of relative source mineral abundances.

(1) Fractional crystallization correction

A least squares regression following Bryan et al. (1968) was used to normalize the lavas to a constant composition. Major element variations in the lavas are suggested to be a result of Rayleigh-type fractionation of olivine or olivine and clinopyroxene in the melt. It is assumed that these lavas were of approximately the same major element composition when generated in the mantle. This implies melting at quasi-invariant and possibly eutectic-like compositions (Feigenson et al., 1983).

In order to generate a primary magma, compositions were calculated by adding enough olivine and clinopyroxene to the samples to create a basalt with 12.4% MgO. The amount of MgO was determined by the sample with the highest MgO content (sample 1-3). Errors in the assumed MgO content of the primary melt have no effect on the inverse modeling because of the low partition coefficients for the REE in olivine. Appendix II contains the data resulting from correction for fractional crystallization.

The selection of minerals used in fractionation-correction was aided by the presence of olivine and clinopyroxene phenocrysts in the thin sections. Both the raw data set and data corrected for fractional crystallization are presented because the raw data only required between 1.2% and 21.6% correction for olivine and clinopyroxene. The calculations for fractionation may be primitive but are usually sufficient. Their purpose is to give the REE concentrations a first-order correction, hence the minimum number of phases was used.

(2) Process identification and source homogeneity testing

Equations by Shaw (1970) were used in process identification and are explained in detail by Hofmann and Feigenson (1983). The main equation is

$$\frac{C^H}{C^i} = S^i C^H + I^i$$

where C^H = a highly incompatible (hygromagmatophile) element, here La, and C^i = concentration of element i. S^i and I^i are the slope and intercept of the straight line described by the above equation. The uncorrected and corrected REE data are shown respectively in Figures 10A and 10B, process identification diagrams of La/C^i versus La. Data points on these plots form straight lines with minimal scatter as is demonstrated by their regression values in Tables 3A and 3B. The different slopes of these lines are a function of the bulk partition coefficients and are caused by the variations in the REE concentrations. The intercepts give information about the initial concentration of each element relative to the source concentration of La. As the intercept approaches

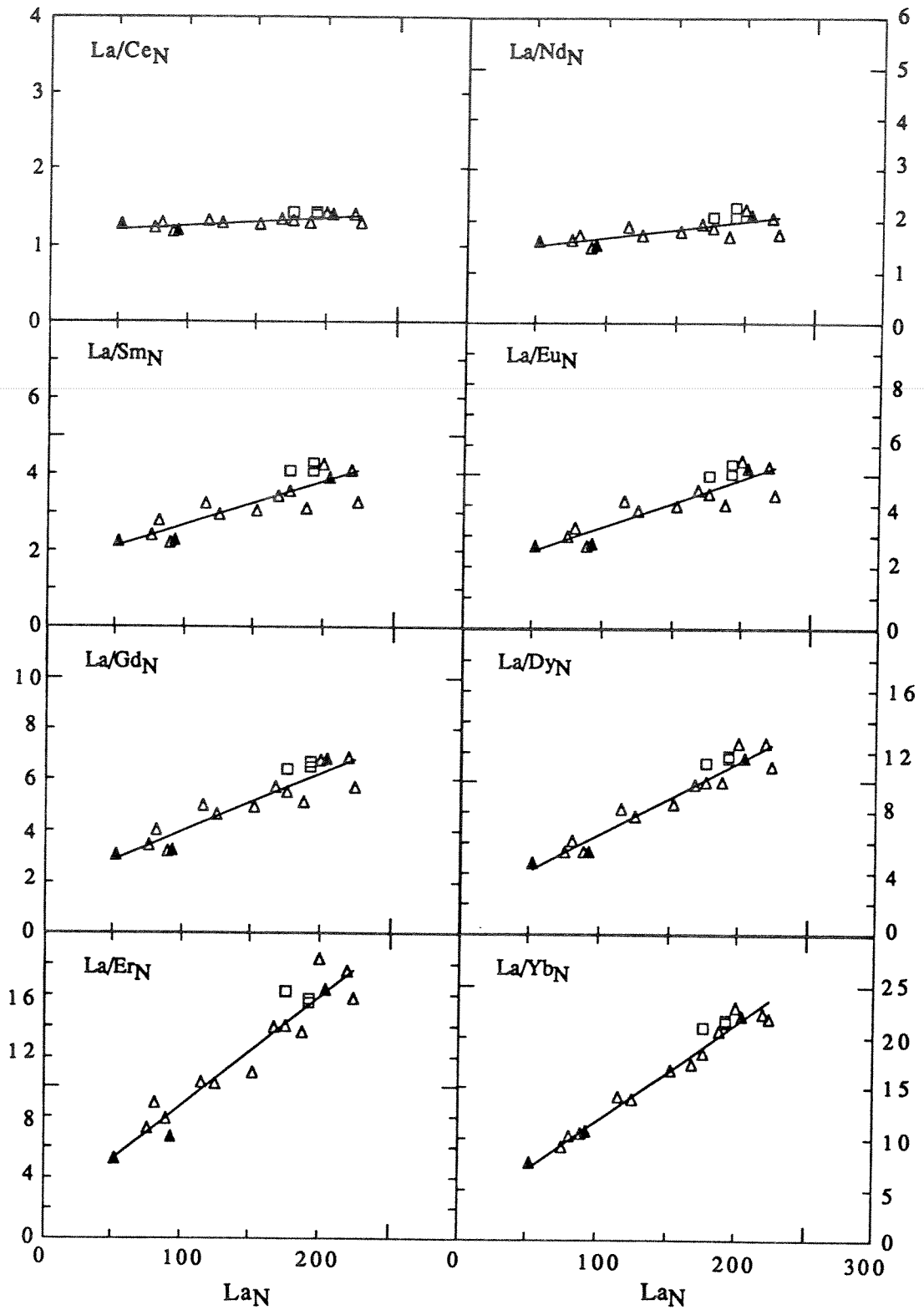


Fig. 10A, B. Process identification diagrams. Slopes increase from light to heavy REE. A. Uncorrected data. Open triangles = PSQ-21; solid triangles = PSQ-24; open squares = samples from along the road.

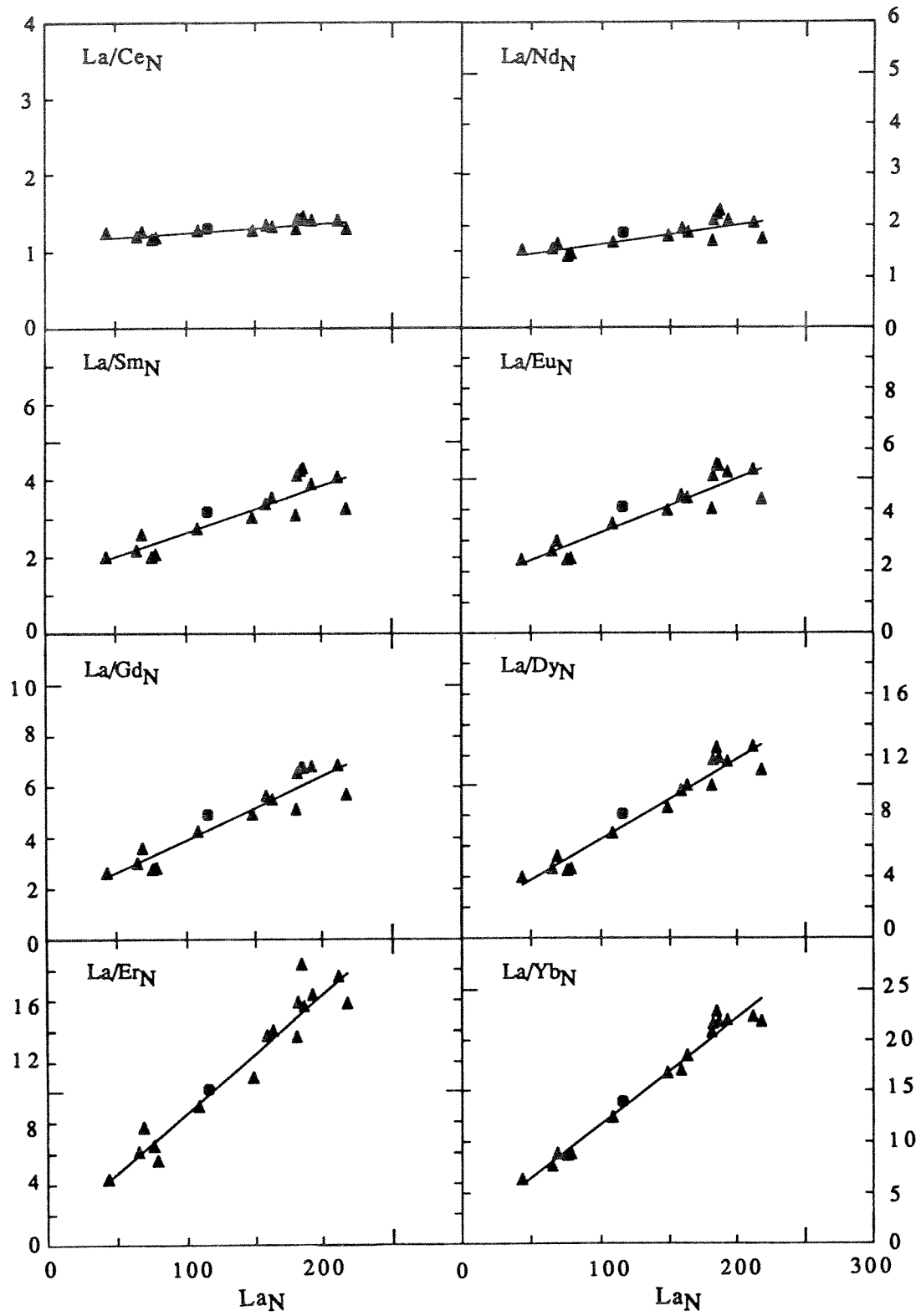


Fig. 10B. Corrected data. Solid triangles = core samples; solid circle = sample with the highest wt.% MgO.

Table 3A. Slopes and intercepts from the process identification diagrams of uncorrected data.

La[N] vs	Slope	+/-	Intercept	+/-	R
La/Ce[N]	0.0010	0.26E-03	1.1404	0.030	0.717
La/Nd[N]	0.0032	0.76E-03	1.3421	0.087	0.724
La/Sm[N]	0.0113	1.80E-03	1.5246	0.207	0.844
La/Eu[N]	0.0159	2.05E-03	1.7067	0.236	0.888
La/Gd[N]	0.0229	2.50E-03	1.6761	0.287	0.916
La/Dy[N]	0.0480	3.41E-03	1.7303	0.390	0.962
La/Er[N]	0.0717	5.46E-03	1.5139	0.626	0.956
La/Yb[N]	0.0962	4.41E-03	2.1112	0.506	0.983

Table 3B. Slopes and intercepts from the process identification diagrams using data corrected for fractional crystallization.

La[N] vs	Slope	+/-	Intercept	+/-	R
La/Ce[N]	0.0012	0.25E-03	1.1142	0.025	0.783
La/Nd[N]	0.0037	0.78E-03	1.2728	0.078	0.771
La/Sm[N]	0.0124	1.79E-03	1.3780	0.178	0.873
La/Eu[N]	0.0177	2.14E-03	1.4770	0.213	0.905
La/Gd[N]	0.0254	2.56E-03	1.3596	0.254	0.931
La/Dy[N]	0.0530	3.61E-03	1.1305	0.358	0.966
La/Er[N]	0.0773	5.56E-03	0.9021	0.553	0.963
La/Yb[N]	0.1049	4.69E-03	1.1814	0.467	0.985

zero, the element approaches its initial concentration. The straight lines formed by the data suggest that the suite of samples was produced by different degrees of melting of identical batches of source material. This is true given the condition of all samples having the same melt partition coefficient (P_i), in other words melting occurs under invariant conditions (Hofmann and Feigenson, 1983). Other processes would cause scatter of data points. Variation in the degree of melting is also suggested by the increasing trend in the La versus MgO plot in Fig. 11 where La increases 4-fold and MgO increases only a small amount.

The equation for C^H/C^i may also be used to test whether the data set could be cogenetic. Positive results occur when REE concentrations on a plot of La/C^i versus La form a line. Two other tests for a uniform source are 1) constant concentration ratios for all hygromagmatophile elements of the suite and 2) constant radiogenic-isotope abundances (Hofmann and Feigenson, 1983).

(3) Calculation of relative concentrations in the initial source

In order to calculate relative concentrations in the initial source, bulk partition coefficients of the melt (P_i) for each REE must be calculated. Partition coefficient P_i is equal to the sum of the equilibrium (mineral/melt) partition coefficients (D_i) of element i weighted proportionately to the consumption of the mineral by the melt. The mineral/melt partition coefficients used are listed in Table 4. The phase assemblage assumed in the calculations is olivine-orthopyroxene-clinopyroxene-garnet. The partition coefficients for olivine and orthopyroxene are very small and are therefore considered inert phases in these calculations.

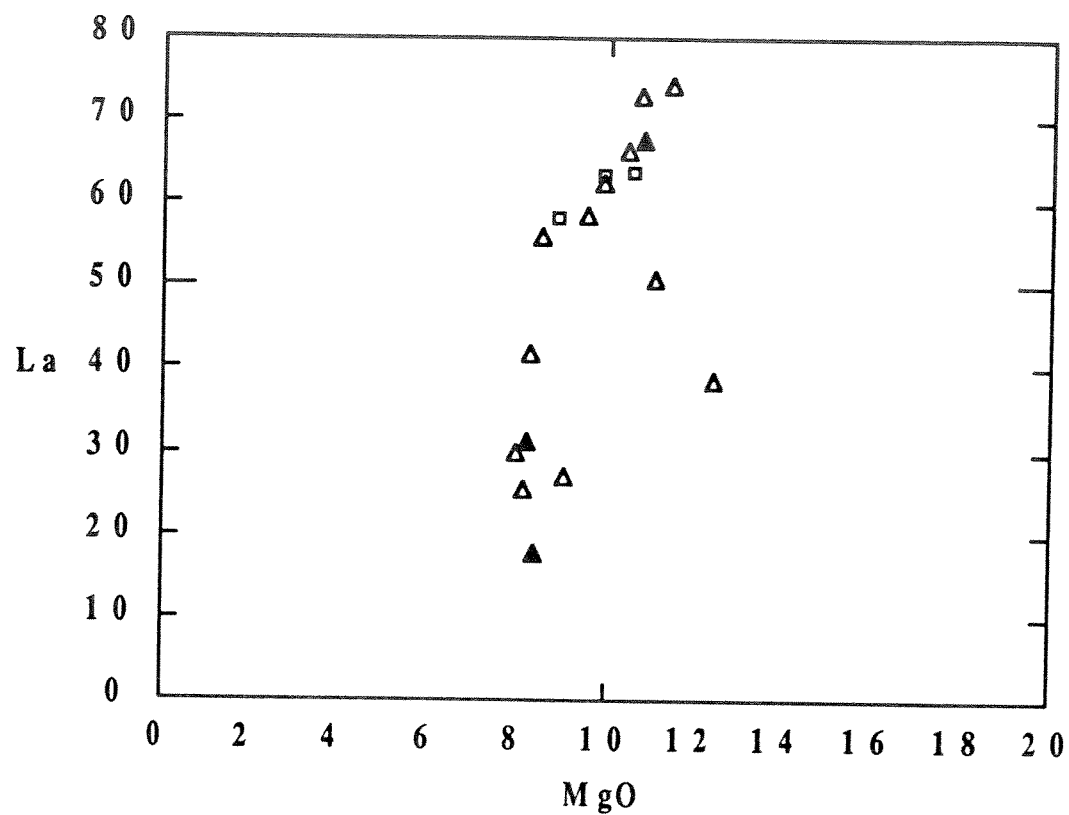


Fig. 11. Lanthanum-magnesia variation diagram. Open triangles = PSQ-21; solid triangles = PSQ-24; open squares = samples from along the road.

The four sets of mineral proportions used to encompass the range of reasonable P_i s are 89%ol+opx-10%cpx-1%gt, 80%ol+opx-0%cpx-20%gt, 10%ol+opx-80%cpx-10%gt and 60%ol+opx-20%cpx-20%gt (Figs. 12A and 12B). Reasonable P_i values are defined here as those that produce relative source concentration and relative bulk partition coefficient patterns with positive numbers.

Table 4. Partition coefficients*

Element	Olivine	Ortho- pyroxene	Clinopyroxene	Garnet
La	0	0.003	0.05	0.01
Ce	0	0.006	0.09	0.02
Nd	0	0.009	0.22	0.09
Sm	0	0.012	0.40	0.22
Eu	0	0.015	0.48	0.33
Gd	0	0.017	0.54	0.50
Dy	0	0.025	0.60	1.06
Er	0	0.035	0.57	2.15
Yb	0	0.050	0.50	4.00

*Compiled from Shimizu and Kushiro (1975) for garnet, Nicholls and Harris (1980) for clinopyroxene, others from Hanson (1980), Irving (1978), and Schnetzler and Philpotts (1970).

A range of possible relative REE source concentrations were then calculated in terms of the measured values of I_i and the calculated P_i values in the equation

$$\frac{C_o^i}{C_o^{La}} = \frac{(1-P_i)}{I_i}$$

The source concentrations of i are not assumed, but are calculated relative to the source concentration of element (La) which is assumed to be equal to one. This makes the shapes of the REE patterns important, rather than their calculated numerical values.

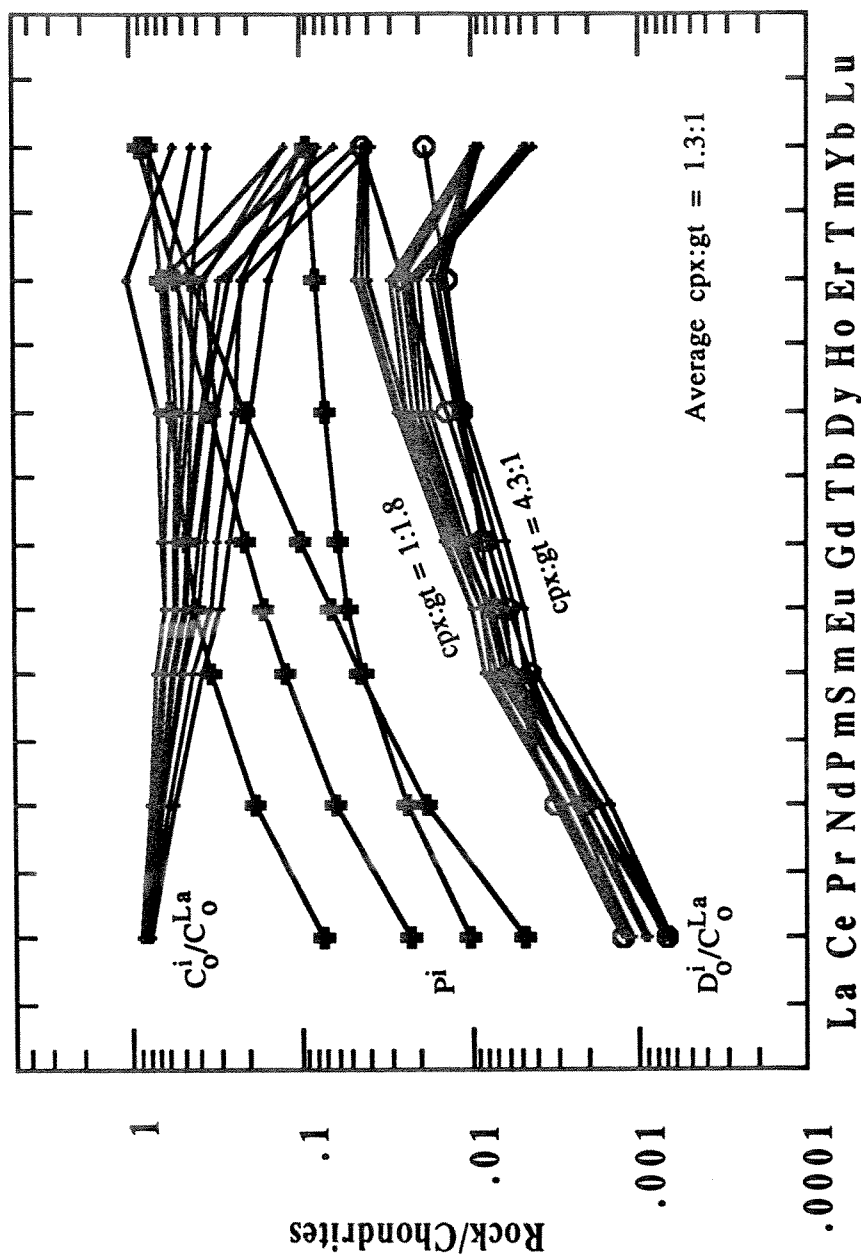


Fig. 12A, B. Bulk partition coefficients, P^i , of the melt (computed from the mineral-melt coefficients given in Table 4 and weighted by the consumption of the minerals by the melt), relative source concentrations $C_0^{La}/C_0^{La} = (1-P^i)/I^i$, and relative bulk partition coefficients of the source assemblage $D_0^{La}/C_0^{La} = S^i(1-P^i)/I^i$. The error bars are propagated from the uncertainty of the S and I values (Table 3) only, because the uncertainties of the P values are unknown. A. Uncorrected data.

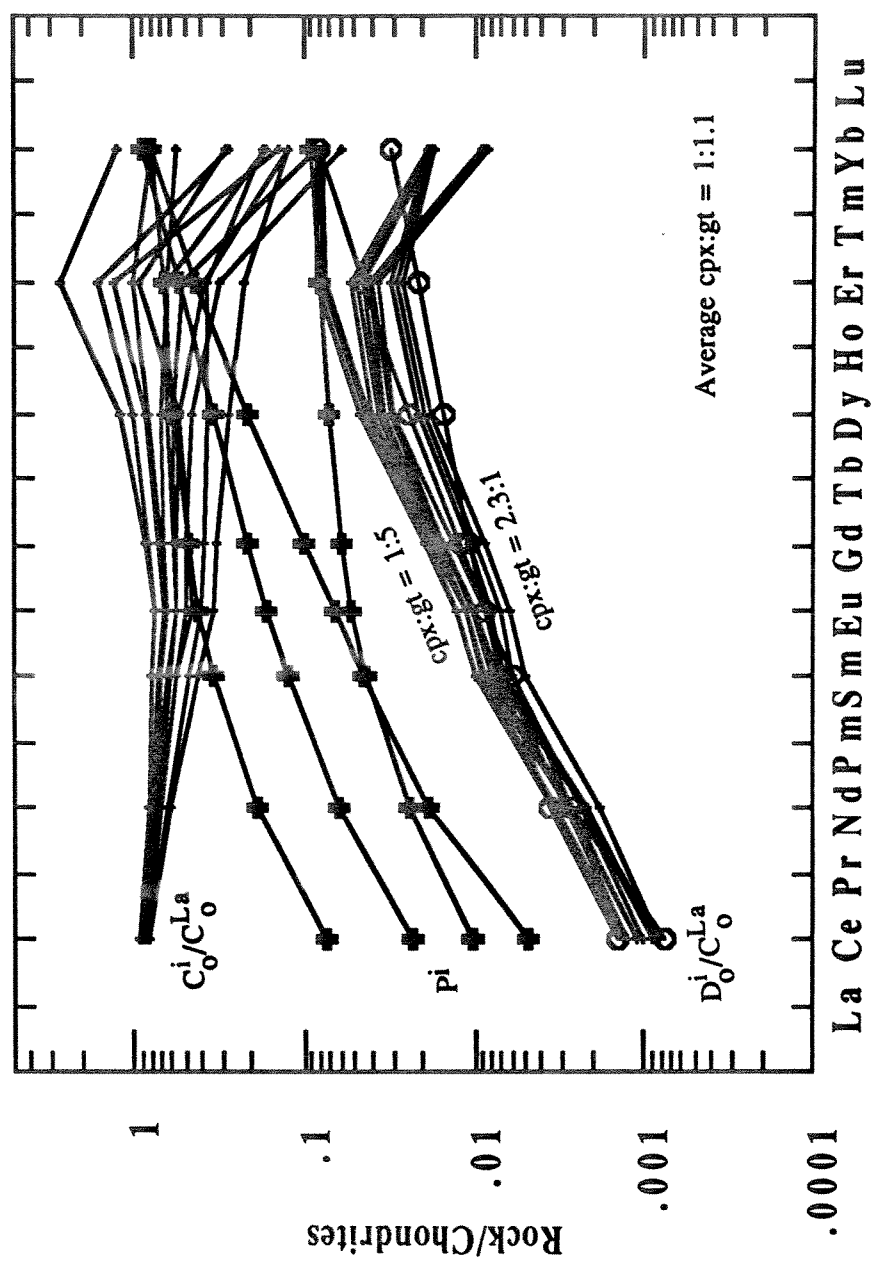


Fig. 12B. Corrected data.

The results of these calculations for both uncorrected and corrected data are shown in Figures 12A and 12B.

For comparison, source patterns from the uncorrected data have been superimposed on a range of REE patterns from spinel lherzolites from Kilbourne Hole, New Mexico (Figure 13). The superimposed data have assumed La concentrations equal to one, therefore it could actually be placed higher or lower on the diagram. The shapes of the spinel lherzolite patterns range from relatively flat to light REE depleted. The patterns of the data presented here are slightly to moderately light REE enriched.

(4) Estimation of relative source mineral abundances

Relative bulk partition coefficients used to estimate relative source mineral abundances were calculated from the equation

$$\frac{D_o^i}{C_o^{La}} = \frac{S^i(1-P^i)}{I^i}$$

By summing the weighted partition coefficients (Table 4) for clinopyroxene and garnet for each element, curves were matched to the highest and lowest possible slopes of the relative bulk partition coefficient range. The weighting of the clinopyroxene and garnet was done on a trial and error basis until the best curve-fit was found. Residual garnet and clinopyroxene was chosen for the melt model because they are believed to be the major potential causes of REE fractionation during melting in the mantle (Feigenson et al., 1983). Matching the high and low slopes bracketed the clinopyroxene to garnet ratios possible in the source (Figs. 12A and 12B). An average curve through the middle of the uncorrected

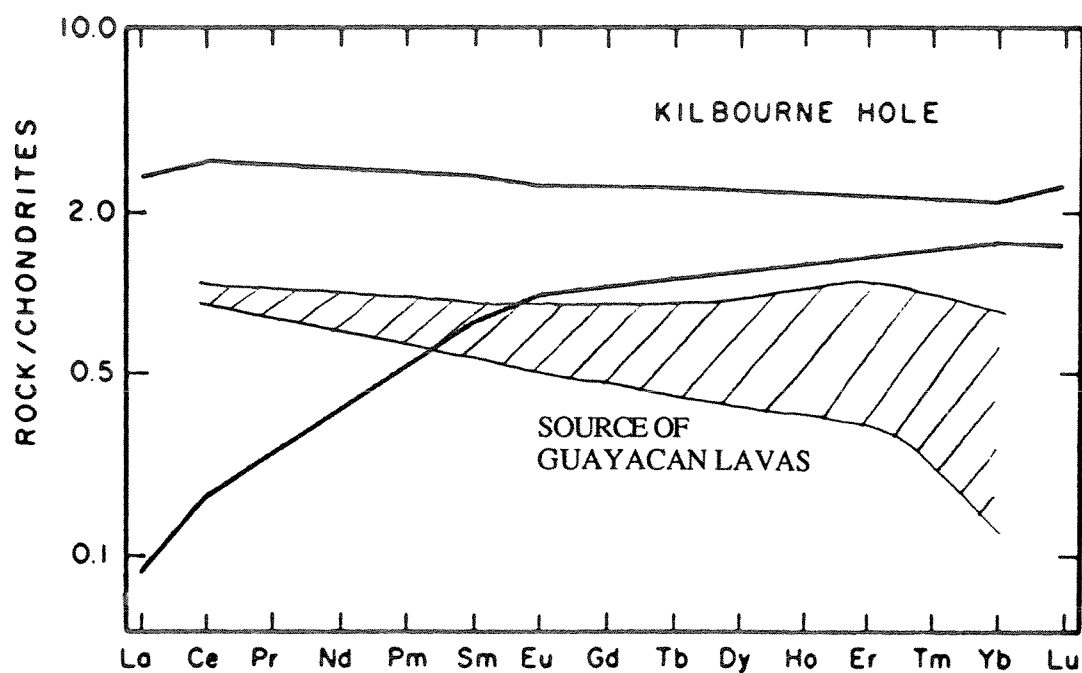


Fig. 13. Range of REE abundances in spinel lherzolites from Kilbourne Hole, New Mexico and Guayacan lavas. (BVTP, 1981).

data range indicates clinopyroxene exceeds garnet in the source by a factor of 1.3. The range of possible clinopyroxene to garnet ratios for the uncorrected data is between 1:1.8 and 4.3:1. An average curve for corrected data produces a clinopyroxene to garnet ratio close to 1:1. The range for corrected data was calculated to be between 1:5 and 2.3:1.

B. Rayleigh Melting Model

Inverse modeling assumes batch melting which is only one end member of possible melting models. The other end member, Rayleigh melting, is explored here as a feasible melting model. Rayleigh melting occurs when melt is continuously extracted from a changing source.

There are two steps used in the Rayleigh melting model. In the first step, source concentrations are calculated using the lava with the lowest measured light REE concentrations (assumed to be from the highest percent melts). In the second step, these calculated source concentrations and smaller degree melts are used to match the curve of the lava with the highest measured light REE concentrations (assumed to be from the lowest percent melts).

The equation used to calculate enrichment factors ($C_i^{\text{melt}}/C_i^{\text{o}}(\text{solids})$) for both steps is from Wood and Fraser (1976):

$$\frac{C_i^{\text{melt}}}{C_i^{\text{o}}(\text{solids})} = \frac{1}{F} \left[1 - \left(1 - \frac{P}{D_o} \right)^{1/P} \right]$$

where F is the percent melt, P is the bulk partition coefficient of the melt, and D_o is the mineral/melt partition coefficient of the source for element i. The first enrichment factors were calculated

using 4% melt because the Guayacán lavas used were estimated to have a high melt of 4%. In Rayleigh melting, P and D values are calculated using assumed amounts of residual olivine (ol), orthopyroxene (opx), clinopyroxene (cpx), and garnet (gt). Source concentrations (C_o) were calculated for each element by dividing measured concentrations (C) from the low light REE (LREE) Guayacán lavas by the first calculated enrichment factors. Enrichment factors were calculated again, but with a smaller degree of melting. Lava concentrations were then calculated by multiplying these second enrichment factors by the calculated source concentrations. By trial and error, the best match of the measured to calculated high LREE lava concentrations was found.

Two different sets of P and D values were used in this melting model. The first set used P values calculated from 50% ol+opx, 40% cpx, and 10% gt, and D values from 75% ol+opx, 20% cpx, and 5% gt (cpx:gt = 4:1). The second set used P values calculated using 89% ol+opx, 10% cpx, and 1% gt, and D values using 94.5% ol+opx, 5% cpx, and 0.5% gt (cpx:gt = 10:1). Both sets used 4% as their high degree of melting and 0.1% melting for their "best" match. Results of these two sets of calculations are presented in Figures 14 and 15, respectively. Referring to Fig. 14 (cpx:gt = 4:1), it is seen that even with a melt as low as 0.1%, the REE concentrations are not even close to the highest LREE lava curve. A better match is found with the cpx:gt = 10:1 (Fig. 15), however, the middle rare earth elements are too low and La and Ce are very high. It may be concluded that the Rayleigh melting model may produce a reasonable source for an individual lava, but cannot

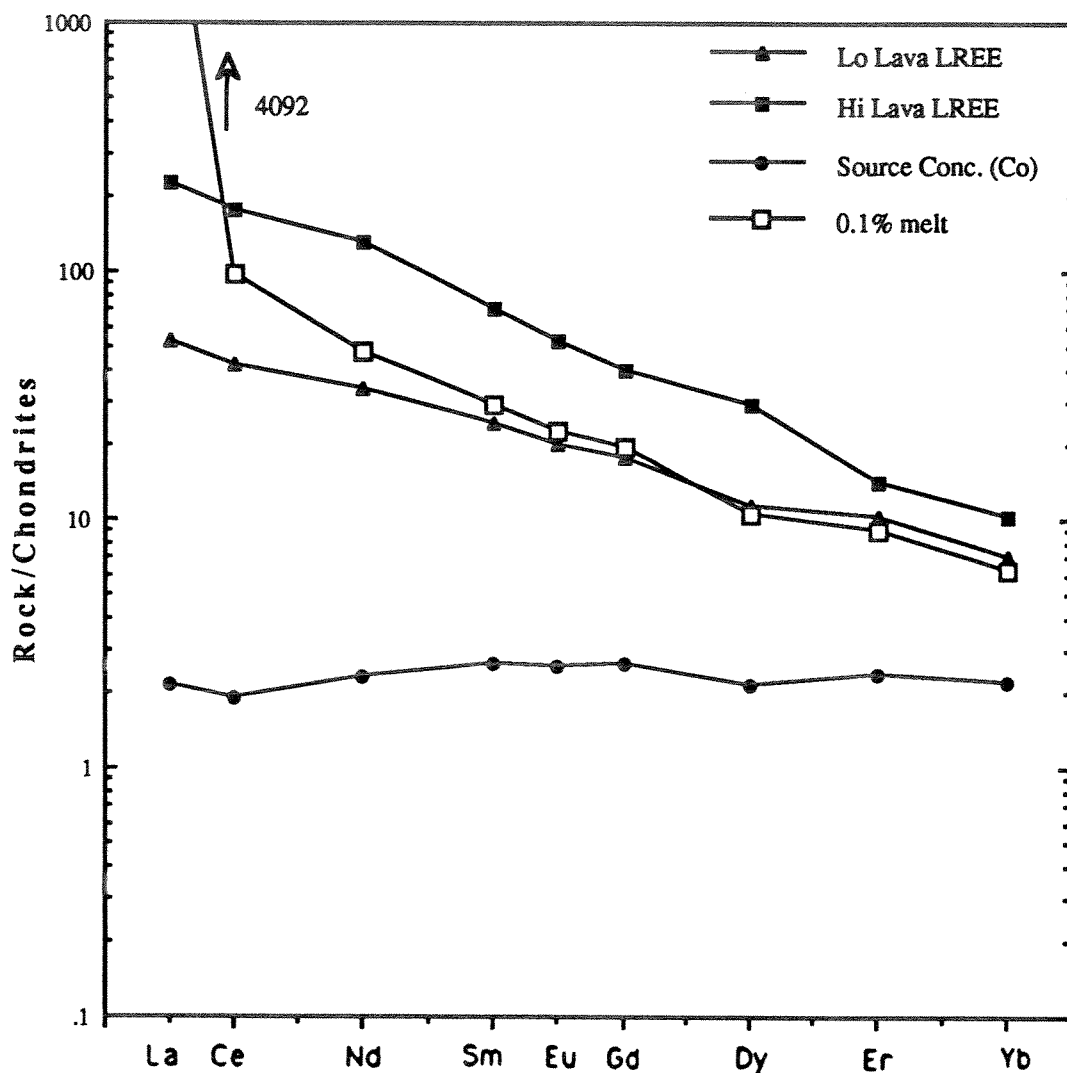


Fig. 14. REE patterns for fractional melting model. Average initial melt is 4%, cpx:gt = 4:1. Partition coefficients for the melt (P) are calculated using 50% ol+opx, 40% cpx, 10% gt. Partition coefficients for the source (D) are calculated using 75% ol+opx, 20% cpx, 5% gt.

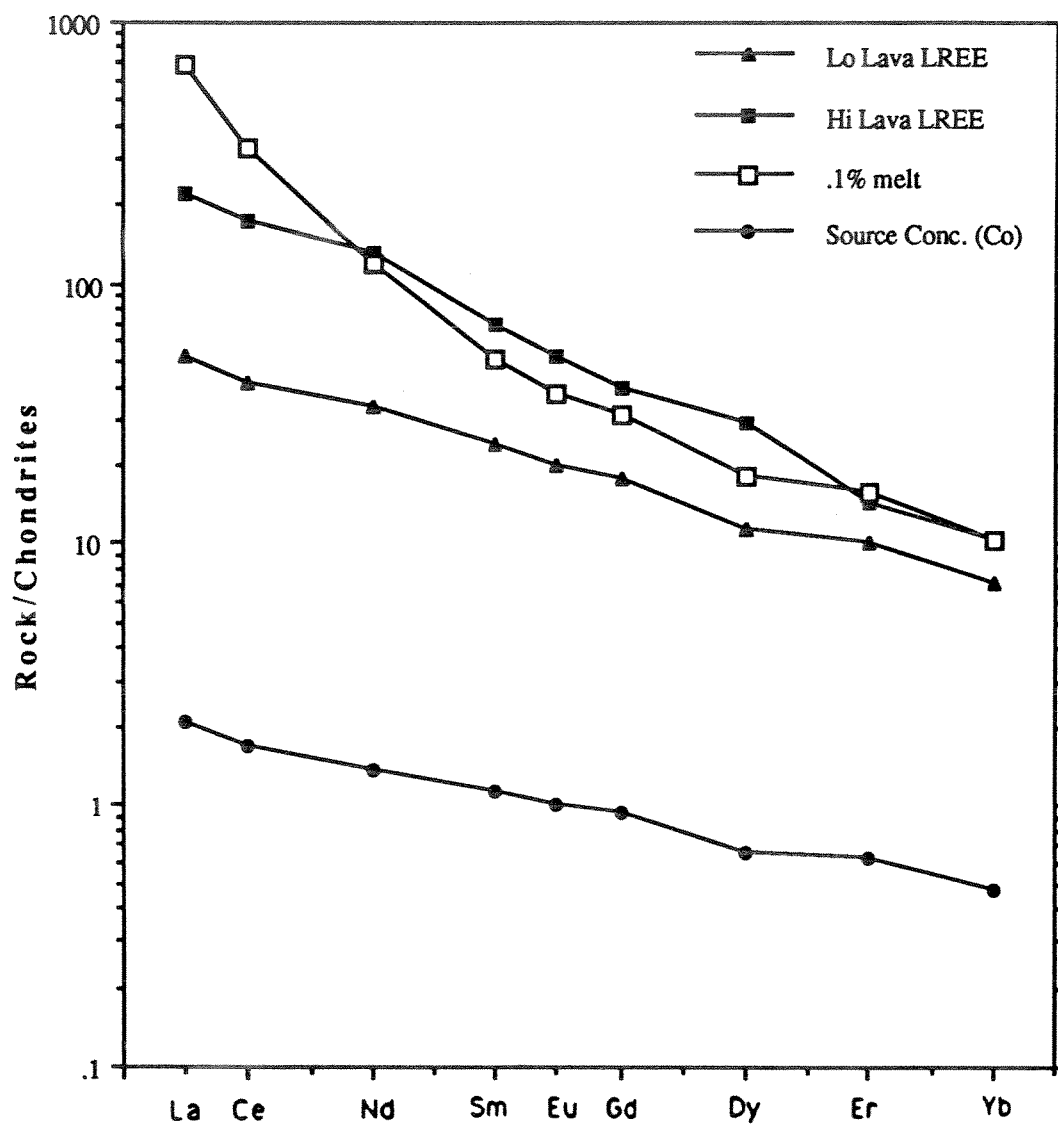


Fig. 15. REE patterns for fractional melting model. Average initial melt is 4%, cpx:gt = 10:1. Partition coefficients for the melt (P) are calculated using 89% ol+opx, 10% cpx, 1% gt. Partition coefficients for the source (D) are calculated using 94.5% ol+opx, 5% cpx, 0.5% gt.

match the observed range of lava compositions from the calculated source. This leads to the investigation of "blended variable batch melting", a model in between that of batch and Rayleigh melting models.

C. Blended Variable Batch Melting Model

Unlike batch or Rayleigh melting, blended variable batch melting is envisioned as occurring when a homogeneous source is melted to varying degrees. The melted material is then thought to rise and mix as it pools together. The mixing creates an average percent melt dependent upon the weight of each different percent melt.

Watson and McKenzie (1990) proposed a numerical model which involved the melting of an axisymmetric mantle plume underlying the Hawaiian swell. I wrote a computer program based on their model that uses a mantle plume where there are variable degrees of melting. Examples of variable melting include plumes with higher degree melts in the center than the edges and plumes with higher degree melts at the top than the bottom. Although plumes are three dimensional, the program was written for a two dimensional slice through the center of a plume. The simple model used here has an average of 4% melts; 0% melt on the outside of the plume, increasing linearly by 0.2%, until a total of 8.0% melt is reached in the center.

The program has two parts which are very similar to the two steps of the Rayleigh melting model. The first part calculates source concentrations using the lava with the lowest measured LREE concentrations. The second part finds a best-fit curve of the

lava with the highest measured LREE concentrations using the calculated source concentrations and smaller degree melts. Lavas suitable for the blended variable batch melting model must be cogenetic and have varying REE concentrations, such as the Guayacán lavas used here.

Part one of the program involves calculating source concentrations. Source concentrations for the REE were calculated using residual olivine, orthopyroxene, clinopyroxene, and garnet. The amounts of cpx and gt used were input into the program and automatically decreased 0.1% for every 0.2% increase in the melt model. The residual ol and opx were added equally to cpx and gt to total 100%. A bulk partition coefficient (D) was calculated by adding the products of the weighted residual minerals and their corresponding partition coefficients (Table 4). It was calculated for each element for each increment in percent melt. An enrichment factor (EF) was then calculated for each D using this formula from Shaw (1970)

$$EF = \frac{1}{D+F-(D \times F)}$$

where F is the percent melt. A total enrichment factor (EFT) was calculated by summing the EFs, weighted by their percent melt. Source concentrations (C_o) were finally calculated for each element by dividing measured concentrations (C) from the lavas by the calculated EFT. Results of these calculations are shown in Fig. 16.

Part two involves using the source concentrations calculated in part one and smaller degree melts to match the highest LREE

curve from the suite of lavas. The results of this part of the program are lava concentrations (C), calculated by multiplying the source values from part one (C_0) by EFT for each element. Matching the high LREE curve is achieved by trial and error and by only lowering the average percent melt. The amount of clinopyroxene and garnet used in part one must also be used in part two. If lowering the percent melt does not provide a reasonable match, new source concentrations using different amounts of clinopyroxene and garnet may need to be calculated.

Figure 16 illustrates the results of both part one (C_0) and part two (0.24% melt) using an initial average of 4% melt and ten times more residual clinopyroxene than garnet. Given these conditions, a reasonable match was found using the "blended variable batch melting" model. The source pattern from this match indicates a light REE enriched source, similar to that of the batch partial melting model in inverse modeling. The ability to match REE patterns using this model may suggest that melting in the mantle could be more like the variable melting rather than the Rayleigh melting or even the batch melting.

V. SUMMARY AND CONCLUSIONS

Major and rare earth element analyses were used in a simple model of batch partial melting, followed by fractional crystallization, to determine mantle source characteristics for a suite of alkaline basalts from the Formación Alkalina de Guayacán. The degree of melting is very small, from less than 0.5% to 4%, based on an assumed source La concentration of 0.66 ppm. The lavas were corrected for fractional crystallization using olivine and

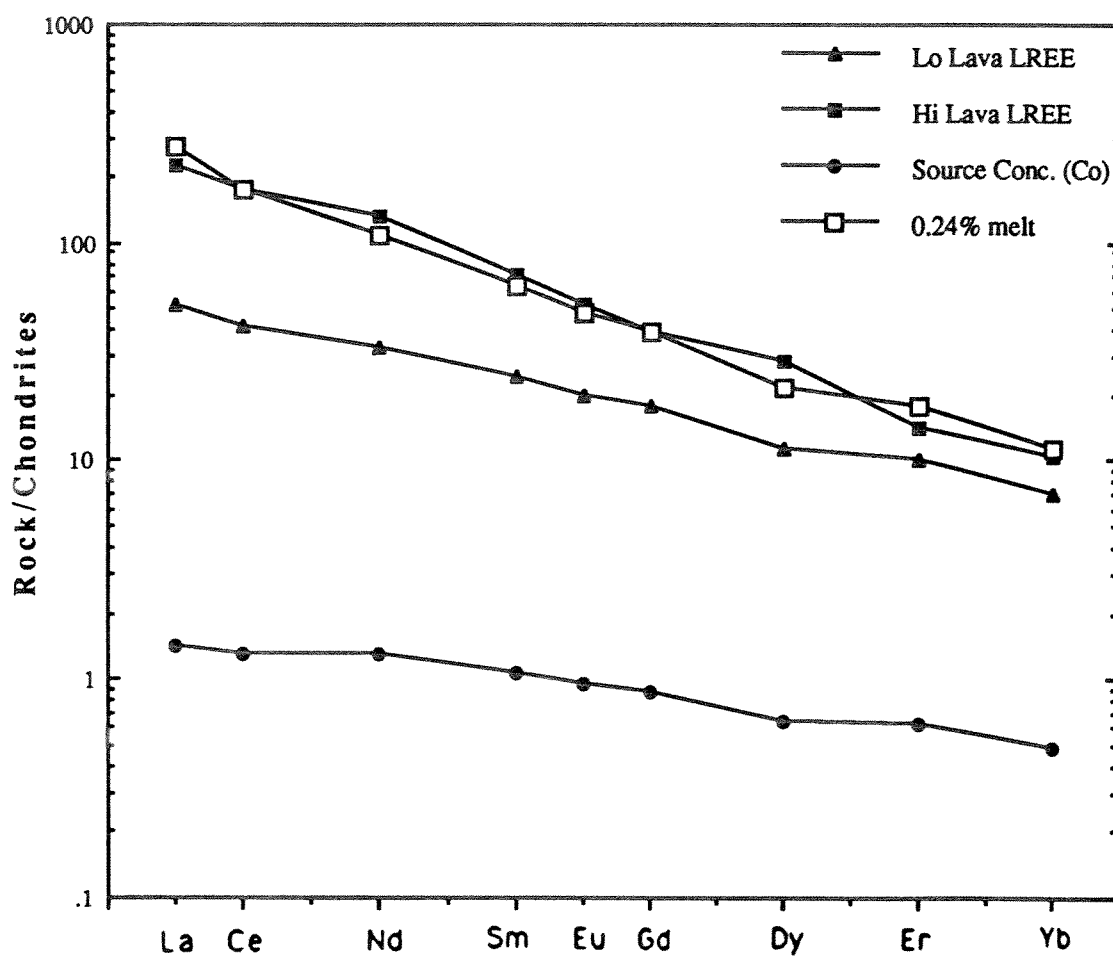


Fig. 16. REE patterns for blended variable batch melting model. Average initial melt is 4%, cpx:gt = 10:1.

clinopyroxene. Because the amounts of correction were small, however, both the uncorrected and corrected data were modelled. The suite of samples have nearly identical Sr and Nd isotopes, implying the source homogeneity needed for inverse modeling. Mean isotope values are 0.703570 and 0.512965 for Sr and Nd, respectively.

A wide range of possible melt partition coefficients was used in inverse modeling to calculate ranges of source concentrations and bulk partition coefficients relative to the incompatible element Lanthanum. The shape of the REE source-concentration patterns for both uncorrected and corrected data indicate a moderately LREE enriched source. The data for relative source bulk partition coefficients suggest that approximately equal amounts of clinopyroxene and garnet are required in the source. Using the results from both uncorrected and corrected data, ratios of clinopyroxene to garnet have limits of 1:5 and 4.3:1, and an average of 1:1.

In using inverse modeling, it is assumed that magma is generated by batch partial melting as opposed to the other generally accepted magma melting model of Rayleigh melting. A Rayleigh melting model was used unsuccessfully in forward modeling even with reasonable source REE concentrations, similar to those of the inverse modeling. The REE patterns did not produce adequate matches to the measured Guayacán lava patterns. More recent thinking by authors such as Thompson (1987) and McKenzie and Bickle (1988) includes variable amounts of melting in the mantle. This idea of a blend of batch and fractional melting is

possibly a more realistic approach than the two end member models. The "blended variable batch melting" model posed here is an attempt to combine the two end member models. The REE source pattern calculated using this variable type of melting is also similar to the source pattern for inverse modeling. The curve produced from forward modeling has proven that it is a viable possibility as a mantle melt model. However, in order to match the observed lava concentrations, the source in the "blended variable" model must have very low garnet compared to clinopyroxene, whereas the batch melting model allows nearly equal garnet and clinopyroxene in the initial source. The models presented here could be applied to other lava suites with the requisite variations in degree of melting, coupled with source homogeneity.

APPENDIX I

Whole Rock Analyses

File name	tina.ROC					
Sample	1-1	1-2	1-3	1-4	1-5	1-6
VN #	89.00	89.00	89.00	89.00	89.00	89.00
Qual	1	1	1	1	1	1
Key	1	1	1	1	1	1
Ref	40	40	40	40	40	40
SiO ₂	41.23	44.82	46.04	42.49	48.55	44.04
TiO ₂	2.12	2.29	1.70	2.48	2.26	2.63
Al ₂ O ₃	14.18	13.32	13.67	12.65	14.64	15.22
FeO	9.51	10.18	9.87	10.22	9.47	10.29
MnO	0.19	0.16	0.16	0.17	0.15	0.16
MgO	9.67	11.08	12.44	11.44	8.28	7.78
CaO	8.09	11.11	9.29	12.03	8.84	8.15
Na ₂ O	1.61	2.16	2.16	1.98	3.28	2.35
K ₂ O	1.06	1.38	1.09	1.47	1.42	0.94
P ₂ O ₅	0.92	0.92	0.70	1.37	0.90	0.73
Total	88.57	97.42	97.12	96.30	97.78	92.29
Rb	12.5	28.5	23.4	30.6	26.1	21.3
Ba	665.6	583.1	564.8	803.9	557.8	613.1
Sr	773.8	2328.0	1226.0	1885.0	1202.0	1085.0
V	215.5	235.7	208.5	291.6	258.4	207.5
Cr	244.9	352.2	382.4	349.0	260.4	151.5
Ni	179.5	246.7	336.4	227.1	177.6	156.1
Zr	211.1	208.6	158.7	175.8	189.6	217.8
Sc	21.3	23.1	23.1	26.2	22.4	18.8
Cu	65.8	77.4	89.2	95.1	76.9	63.3
La	0.00	50.53	38.15	73.92	41.58	0.00
Ce	0.00	105.40	76.95	152.10	86.08	0.00
Nd	0.00	55.03	39.49	82.58	46.78	0.00
Sm	0.00	10.42	7.36	14.20	8.89	0.00
Eu	0.00	2.99	2.17	4.02	2.58	0.00
Gd	0.00	8.69	6.50	10.95	7.58	0.00
Dy	0.00	6.23	4.87	7.03	5.66	0.00
Er	0.00	3.18	2.54	3.22	2.79	0.00
Yb	0.00	2.02	1.82	2.27	2.01	0.00
Y	0.00	29.70	24.69	33.74	28.50	0.00
Strat	1	2	3	4	5	6
FeO*	9.51	10.18	9.87	10.22	9.47	10.29
Mg#	64.46	66.01	69.22	66.63	60.93	57.42
Density	2.74	2.75	2.73	2.79	2.68	2.71

Sample	1-7	1-7A	1-8	1-9	1-10	1-11
VN #	89.00	89.00	89.00	89.00	89.00	89.00
Qual	1	1	1	1	1	1
Key	1	1	1	1	1	1
Ref	40	40	40	40	40	40
SiO ₂	44.11	43.03	48.54	45.10	46.41	45.97
TiO ₂	2.28	2.22	2.03	1.74	2.72	2.77
Al ₂ O ₃	14.26	13.48	15.23	14.22	13.92	14.05
FeO	10.64	10.50	9.10	7.84	10.40	10.42
MnO	0.17	0.17	0.14	0.12	0.16	0.17
MgO	9.58	9.90	8.92	8.30	10.00	9.49
CaO	10.61	11.33	9.59	7.32	10.73	11.27
Na ₂ O	3.45	1.87	2.81	1.46	2.37	2.51
K ₂ O	1.53	1.01	1.61	1.07	1.48	1.19
P ₂ O ₅	1.15	1.13	0.76	0.56	1.08	1.13
Total	97.78	94.64	98.73	87.74	99.27	98.97
Rb	25.2	22.1	32.1	13.7	28.5	29.7
Ba	701.8	936.3	629.1	541.5	659.2	671.9
Sr	1533.0	2861.0	1111.0	1510.0	1461.0	2279.0
V	240.6	233.1	253.0	184.0	267.5	273.6
Cr	225.6	243.9	225.5	205.8	293.6	289.8
Ni	185.1	188.6	145.2	145.4	195.5	193.4
Zr	167.5	158.6	178.5	149.8	191.1	193.6
Sc	22.1	22.1	24.2	21.3	24.0	25.4
Cu	88.8	89.0	86.5	87.2	114.2	119.1
La	0.00	61.90	0.00	0.00	0.00	58.14
Ce	0.00	127.90	0.00	0.00	0.00	116.70
Nd	0.00	70.67	0.00	0.00	0.00	60.33
Sm	0.00	12.46	0.00	0.00	0.00	10.17
Eu	0.00	3.64	0.00	0.00	0.00	3.14
Gd	0.00	10.21	0.00	0.00	0.00	8.91
Dy	0.00	6.53	0.00	0.00	0.00	6.13
Er	0.00	3.13	0.00	0.00	0.00	2.86
Yb	0.00	2.01	0.00	0.00	0.00	2.12
Y	0.00	31.77	0.00	0.00	0.00	30.47
Strat	7	7	8	9	10	11
FeO*	10.64	10.50	9.10	7.84	10.40	10.42
Mg#	61.63	62.71	63.62	65.38	63.17	61.90
Density	2.74	2.77	2.68	2.66	2.74	2.74

Sample	1-12	1-13	1-14	1-15	1-16	1-17
VN #	89.00	89.00	89.00	89.00	89.00	89.00
Qual	1	1	1	1	1	1
Key	1	1	1	1	1	1
Ref	40	40	40	40	40	40
SiO2	46.40	46.88	44.68	46.94	45.94	46.31
TiO2	2.28	2.26	1.73	1.99	2.02	2.78
Al2O3	14.27	14.26	13.42	14.16	14.35	15.10
FeO	9.49	9.51	9.31	10.08	9.51	10.15
MnO	0.15	0.16	0.16	0.16	0.16	0.15
MgO	8.48	9.16	10.72	10.08	9.74	7.93
CaO	9.80	10.09	11.60	12.25	12.45	8.02
Na2O	2.91	2.84	2.12	2.83	2.03	2.89
K2O	1.49	1.56	1.15	0.95	1.04	1.61
P2O5	1.01	1.02	1.02	0.87	0.99	0.71
Total	96.28	97.73	95.90	100.31	98.22	95.64
Rb	26.7	30.5	19.5	21.1	16.9	30.1
Ba	648.6	686.8	851.5	691.0	779.5	541.7
Sr	1416.0	1906.0	1866.0	1318.0	1536.0	969.3
V	240.7	232.8	230.5	255.5	260.0	219.2
Cr	268.9	240.2	380.8	305.3	316.1	118.7
Ni	187.8	169.0	250.6	205.6	192.1	142.5
Zr	203.8	201.0	182.7	170.2	170.6	219.0
Sc	23.7	24.4	26.0	28.1	27.8	19.5
Cu	110.9	102.1	126.1	117.3	111.9	76.5
La	55.55	0.00	72.52	0.00	0.00	29.61
Ce	110.00	0.00	137.80	0.00	0.00	66.68
Nd	55.63	0.00	68.40	0.00	0.00	38.87
Sm	10.09	0.00	11.05	0.00	0.00	8.41
Eu	2.91	0.00	3.23	0.00	0.00	2.63
Gd	8.23	0.00	8.95	0.00	0.00	7.86
Dy	5.96	0.00	6.06	0.00	0.00	5.80
Er	2.74	0.00	2.84	0.00	0.00	2.60
Yb	2.15	0.00	2.18	0.00	0.00	1.91
Y	29.09	0.00	29.75	0.00	0.00	27.91
Strat	12	13	14	15	16	17
FeO*	9.49	9.51	9.31	10.08	9.51	10.15
Mg#	61.45	63.21	67.26	64.08	64.63	58.22
Density	2.70	2.70	2.74	2.73	2.74	2.69

Sample	1-18	1-19	1-20	1-21	1-22	1-23
VN #	89.00	89.00	89.00	89.00	89.00	89.00
Qual	1	1	1	1	1	1
Key	1	1	1	1	1	1
Ref	40	40	40	40	40	40
SiO2	47.04	45.77	47.68	48.92	43.68	41.13
TiO2	1.77	1.81	1.81	1.88	1.80	1.59
Al2O3	14.98	14.50	14.80	15.22	12.72	13.04
FeO	9.57	9.23	9.56	9.98	9.94	8.10
MnO	0.15	0.15	0.14	0.16	0.16	0.10
MgO	10.43	10.01	8.31	9.06	10.82	7.13
CaO	11.38	10.89	8.50	8.69	10.70	6.99
Na2O	2.98	2.56	3.05	3.03	1.65	2.64
K2O	1.38	1.41	1.29	1.29	1.32	1.21
P2O5	1.02	1.02	0.54	0.53	0.87	0.46
Total	100.70	97.35	95.68	98.76	93.65	82.39
Rb	25.9	26.3	23.5	25.0	33.0	22.5
Ba	703.1	732.9	464.6	470.5	695.5	411.3
Sr	1599.0	1764.0	869.2	846.2	1596.0	752.3
V	245.4	249.3	244.7	248.8	233.3	200.1
Cr	336.9	300.6	234.9	230.8	326.1	154.7
Ni	187.8	181.8	175.3	178.5	228.7	116.5
Zr	141.4	186.3	149.1	147.7	175.4	142.7
Sc	26.8	25.5	24.2	24.2	24.1	20.2
Cu	101.1	100.4	133.4	122.9	103.6	77.7
La	65.93	0.00	0.00	26.76	0.00	0.00
Ce	123.10	0.00	0.00	55.51	0.00	0.00
Nd	57.58	0.00	0.00	30.32	0.00	0.00
Sm	9.62	0.00	0.00	6.00	0.00	0.00
Eu	2.83	0.00	0.00	1.94	0.00	0.00
Gd	8.22	0.00	0.00	5.65	0.00	0.00
Dy	5.52	0.00	0.00	4.60	0.00	0.00
Er	2.47	0.00	0.00	2.07	0.00	0.00
Yb	1.93	0.00	0.00	1.77	0.00	0.00
Y	26.99	0.00	0.00	24.28	0.00	0.00
Strat	18	19	20	21	22	23
FeO*	9.57	9.23	9.56	9.98	9.94	8.10
Mg#	66.04	65.93	60.79	61.82	66.01	61.09
Density	2.72	2.72	2.67	2.68	2.75	2.66

Sample	1-24	4-1	4-2	4-3	4-4	4-5
VN #	89.00	89.00	89.00	89.00	89.00	89.00
Qual	1	1	1	1	1	1
Key	1	2	2	2	2	2
Ref	40	40	40	40	40	40
SiO2	47.30	43.78	45.13	44.25	45.36	47.69
TiO2	1.83	2.53	2.61	2.56	1.74	1.78
Al2O3	14.73	13.37	13.66	13.64	13.39	14.74
FeO	9.71	9.98	10.32	9.86	9.55	10.10
MnO	0.14	0.15	0.16	0.14	0.15	0.16
MgO	8.12	9.22	9.74	9.17	10.77	8.37
CaO	8.18	10.25	10.45	9.58	11.90	9.18
Na2O	3.15	2.34	2.78	2.38	2.18	3.08
K2O	1.20	1.39	1.46	1.46	1.27	1.16
P2O5	0.46	1.07	1.06	1.00	0.96	0.57
Total	94.82	94.08	97.37	94.04	97.27	96.83
Rb	22.8	27.3	26.9	30.0	25.1	20.8
Ba	391.9	725.1	646.3	569.9	809.4	448.3
Sr	753.5	1571.0	1440.0	1131.0	1922.0	943.8
V	239.1	265.9	264.7	245.4	229.3	248.9
Cr	208.8	275.3	282.2	243.0	340.4	199.5
Ni	148.5	197.0	202.1	170.8	228.6	148.4
Zr	152.0	178.3	173.6	232.0	187.7	150.3
Sc	23.4	25.4	25.7	24.1	25.9	23.9
Cu	74.0	114.7	112.0	103.0	120.5	120.4
La	25.08	0.00	0.00	0.00	67.26	0.00
Ce	54.43	0.00	0.00	0.00	127.30	0.00
Nd	29.99	0.00	0.00	0.00	62.28	0.00
Sm	6.61	0.00	0.00	0.00	10.71	0.00
Eu	2.00	0.00	0.00	0.00	3.03	0.00
Gd	6.18	0.00	0.00	0.00	8.36	0.00
Dy	4.92	0.00	0.00	0.00	6.07	0.00
Er	2.39	0.00	0.00	0.00	2.83	0.00
Yb	1.86	0.00	0.00	0.00	2.05	0.00
Y	26.12	0.00	0.00	0.00	27.93	0.00
Strat	24	11	12	13	14	15
FeO*	9.71	9.98	10.32	9.86	9.55	10.10
Mg#	59.86	62.23	62.74	62.39	66.80	59.65
Density	2.67	2.74	2.74	2.73	2.74	2.68

Sample	4-6	4-7	4-8	4-9	4-10	4-11
VN #	89.00	89.00	89.00	89.00	89.00	89.00
Qual	1	1	1	1	1	1
Key	2	2	2	2	2	2
Ref	40	40	40	40	40	40
SiO2	47.97	47.40	46.67	45.25	47.29	47.19
TiO2	1.64	1.66	2.78	1.78	1.78	1.78
Al2O3	15.08	15.56	15.25	14.41	14.87	14.74
FeO	10.47	10.90	10.14	9.12	9.39	9.45
MnO	0.16	0.14	0.14	0.15	0.14	0.15
MgO	7.86	8.39	8.22	10.43	8.03	8.06
CaO	9.00	8.92	8.06	10.87	8.39	8.65
Na2O	2.83	2.49	2.72	2.13	2.87	2.79
K2O	0.69	0.22	1.65	1.27	1.23	1.18
P2O5	0.43	0.31	0.72	1.02	0.55	0.52
Total	96.12	95.98	96.35	96.43	94.53	94.51
Rb	13.2	8.9	34.1	28.1	26.7	24.6
Ba	359.6	194.5	601.8	738.2	450.5	469.7
Sr	881.1	721.8	1012.0	1565.0	805.9	976.3
V	229.6	259.7	227.7	241.3	236.3	243.9
Cr	232.4	199.0	142.8	318.6	218.7	271.9
Ni	179.8	164.8	156.4	188.5	167.2	193.5
Zr	121.2	99.2	235.1	194.0	150.8	144.5
Sc	22.9	23.3	20.1	26.3	23.7	24.3
Cu	159.7	170.1	73.7	99.6	107.5	124.8
La	0.00	17.35	30.85	0.00	0.00	0.00
Ce	0.00	36.25	68.57	0.00	0.00	0.00
Nd	0.00	21.11	39.38	0.00	0.00	0.00
Sm	0.00	4.90	8.52	0.00	0.00	0.00
Eu	0.00	1.54	2.66	0.00	0.00	0.00
Gd	0.00	4.89	8.13	0.00	0.00	0.00
Dy	0.00	3.91	6.01	0.00	0.00	0.00
Er	0.00	2.30	3.19	0.00	0.00	0.00
Yb	0.00	1.56	1.95	0.00	0.00	0.00
Y	0.00	21.14	29.44	0.00	0.00	0.00
Strat	16	17	18	19	20	21
FeO*	10.47	10.90	10.14	9.12	9.39	9.45
Mg#	57.25	57.86	59.12	67.11	60.40	60.34
Density	2.68	2.70	2.69	2.73	2.67	2.67

Sample	4-12	4-13	4-14	T	GU-1	GU-2
VN #	89.00	89.00	89.00	89.00	89.00	89.00
Qual	1	1	1	1	1	1
Key	2	2	2	3	3	3
Ref	40	40	40	40	40	40
SiO ₂	47.56	48.64	48.70	43.74	45.82	45.06
TiO ₂	1.80	1.81	1.94	1.75	1.96	1.82
Al ₂ O ₃	15.02	15.37	15.48	13.81	14.38	13.52
FeO	9.46	9.60	9.39	9.53	9.42	10.08
MnO	0.14	0.15	0.14	0.15	0.15	0.16
MgO	8.20	8.83	7.22	8.87	9.86	10.54
CaO	8.10	8.66	8.23	15.26	10.28	11.77
Na ₂ O	2.92	3.09	3.18	2.66	2.51	2.42
K ₂ O	1.30	1.26	1.39	1.03	1.35	0.93
P ₂ O ₅	0.53	0.53	0.54	0.89	0.89	0.90
Total	95.02	97.94	96.21	97.70	96.62	97.21
Rb	25.2	20.7	23.5	22.1	31.6	23.0
Ba	454.4	486.3	515.5	741.8	678.2	674.6
Sr	761.5	883.2	797.7	1691.0	2134.0	3475.0
V	241.2	261.5	251.7	256.1	232.4	233.0
Cr	230.0	255.8	195.6	178.1	282.8	314.5
Ni	180.3	191.4	136.2	92.6	195.2	221.9
Zr	148.0	153.4	168.1	170.1	190.7	172.4
Sc	23.4	24.8	23.9	37.8	24.1	24.9
Cu	113.4	182.0	86.9	104.4	92.2	106.1
La	0.00	0.00	0.00	58.06	63.40	63.65
Ce	0.00	0.00	0.00	106.70	116.50	119.30
Nd	0.00	0.00	0.00	53.57	53.43	58.33
Sm	0.00	0.00	0.00	8.72	9.13	9.60
Eu	0.00	0.00	0.00	2.73	2.76	2.93
Gd	0.00	0.00	0.00	7.56	7.89	8.17
Dy	0.00	0.00	0.00	5.36	5.62	5.73
Er	0.00	0.00	0.00	2.44	2.79	2.76
Yb	0.00	0.00	0.00	1.85	1.95	1.98
Y	0.00	0.00	0.00	26.06	28.13	27.90
Strat	22	23	24	0	0	0
FeO*	9.46	9.60	9.39	9.53	9.42	10.08
Mg#	60.72	62.13	57.83	62.41	65.12	65.10
Density	2.67	2.67	2.65	2.75	2.71	2.74

Sample	GU-3
VN #	89.00
Qual	1
Key	3
Ref	40

SiO ₂	43.85
TiO ₂	1.77
Al ₂ O ₃	13.18
FeO	9.91
MnO	0.16
MgO	10.63
CaO	10.58
Na ₂ O	1.71
K ₂ O	1.36
P ₂ O ₅	0.86
Total	94.01

Rb	29.9
Ba	695.0
Sr	1550.0
V	234.6
Cr	333.8
Ni	241.3
Zr	176.4
Sc	24.9
Cu	105.0
FeO*	9.91
Mg#	65.68
Density	2.74

APPENDIX II

Whole Rock Analyses Corrected for Fractional Crystallization

File name:ctina3.roc

Sample	1-3	1-2	1-4	1-5	1-7A	1-11
SiO ₂	46.04	45.36	43.15	48.84	44.27	45.87
TiO ₂	1.70	2.22	2.42	2.12	2.13	2.56
Al ₂ O ₃	13.67	12.93	12.32	12.98	12.97	12.99
FeO	9.87	10.41	10.46	9.65	10.92	10.60
MnO	0.16	0.16	0.16	0.14	0.17	0.16
MgO	12.44	13.02	13.30	12.74	13.04	12.91
CaO	9.29	10.79	11.72	9.35	10.90	10.42
Na ₂ O	2.16	2.10	1.93	2.82	1.80	2.32
K ₂ O	1.09	1.34	1.43	1.21	0.97	1.10
P ₂ O ₅	0.70	0.89	1.33	0.76	1.09	1.04
Total	97.1	99.2	98.2	100.6	98.3	100.0
Rb	23	28	30	22	21	27
Ba	565	566	783	475	901	621
Sr	1226	2261	1837	1034	2754	2107
V	208	229	284	241	224	253
Cr	382	344	342	511	237	270
Ni	336	553	580	928	746	685
Zr	159	204	172	166	154	180
La	38.15	49.05	71.99	35.81	59.53	53.72
Ce	76.95	102.32	148.13	75.37	122.99	107.82
Nd	39.49	53.42	80.43	41.74	67.96	55.74
Sm	7.36	10.12	13.83	8.17	11.98	9.40
Eu	2.17	2.90	3.92	2.40	3.50	2.90
Gd	6.50	8.44	10.66	7.18	9.82	8.23
Dy	4.87	6.05	6.85	5.49	6.28	5.66
Er	2.54	3.09	3.14	2.71	3.01	2.64
Yb	1.82	1.96	2.21	1.95	1.93	1.96

File name:ctina3.roc

Sample	1-12	1-14	1-17	1-18	1-21	1-24
SiO ₂	47.94	45.41	47.84	46.32	48.42	48.49
TiO ₂	2.17	1.67	2.60	1.64	1.80	1.80
Al ₂ O ₃	13.49	12.94	13.30	13.86	13.30	13.07
FeO	10.08	9.65	10.24	9.65	9.84	9.88
MnO	0.15	0.15	0.14	0.15	0.15	0.14
MgO	12.76	13.19	12.73	13.07	12.75	12.73
CaO	9.48	11.19	9.50	10.53	9.41	9.40
Na ₂ O	2.74	2.04	2.44	2.76	2.57	2.69
K ₂ O	1.40	1.11	1.33	1.28	1.07	1.01
P ₂ O ₅	0.95	0.98	0.58	0.94	0.44	0.38
Total	101.2	98.3	100.7	100.2	99.8	99.6

Rb	25	19	25	24	21	19
Ba	610	821	449	651	393	329
Sr	1333	1800	815	1480	714	642
V	229	222	210	227	232	230
Cr	284	370	374	314	544	609
Ni	703	784	871	504	846	940
Zr	194	178	188	132	127	132
La	52.27	69.91	24.96	60.98	22.65	21.42
Ce	103.72	132.84	57.73	113.87	47.96	47.65
Nd	52.59	65.94	34.70	53.26	26.82	27.01
Sm	9.58	10.65	7.88	8.90	5.51	6.22
Eu	2.77	3.11	2.52	2.62	1.81	1.92
Gd	7.84	8.63	7.72	7.60	5.38	6.08
Dy	5.70	5.84	5.93	5.11	4.52	5.03
Er	2.62	2.74	2.66	2.28	2.03	2.44
Yb	2.06	2.10	1.95	1.79	1.74	1.90

File name:ctina3.roc

Sample	4-4	4-7	4-8	GU-1	GU-2
SiO ₂	45.32	47.16	47.88	47.12	45.02
TiO ₂	1.64	1.60	2.60	1.90	1.71
Al ₂ O ₃	12.66	13.36	13.41	13.93	12.73
FeO	9.73	10.60	10.17	9.91	10.23
MnO	0.15	0.13	0.13	0.15	0.16
MgO	13.18	12.74	12.75	12.91	13.10
CaO	11.25	9.62	9.49	9.96	11.08
Na ₂ O	2.06	2.08	2.30	2.43	2.28
K ₂ O	1.20	0.18	1.36	1.31	0.88
P ₂ O ₅	0.91	0.26	0.59	0.86	0.85
Total	98.1	97.7	100.7	100.5	98.0
Rb	24	7	28	31	22
Ba	765	159	498	657	636
Sr	1817	599	850	2067	3274
V	217	243	217	225	219
Cr	324	576	440	276	299
Ni	766	1244	880	515	792
Zr	179	84	201	186	164
La	63.55	14.43	26.00	61.38	59.92
Ce	120.28	30.91	59.32	112.79	112.30
Nd	58.85	18.53	35.10	51.73	54.91
Sm	10.12	4.50	7.96	8.84	9.04
Eu	2.86	1.44	2.54	2.67	2.76
Gd	7.90	4.70	7.96	7.64	7.69
Dy	5.74	3.90	6.12	5.44	5.39
Er	2.67	2.29	3.25	2.70	2.60
Yb	1.94	1.56	1.99	1.89	1.86

APPENDIX III

REE Separation Procedure (9/7/90)

1. Backwash columns with 1.5N HCL.
2. Flux 0.2g sample plus 0.5g LiBO₂.
3. Fuse for 15 minutes.
4. Dissolve in 25ml 1.5N HCL (from MDF lab) in teflon TEE (white) 100ml beakers.
5. Put on stirring plate until dissolved (15-30 minutes).
6. Load 25ml solution onto columns, collecting in waste beakers.
7. Let entire 25ml drip through (about 30 minutes).
8. Add 1-2ml 1.5N HCL into each beaker with stir bar still in. Clean up all remaining sample, avoid graphite, add to column (rinse). Repeat as necessary.
9. When rinse drips through add 1.5N HCL up to 50ml total.
10. When 50ml has dripped through (eluted) change to 2.3N HCL.
11. Add 40ml 2.3N HCL to all columns. Add 50ml to columns 3 and 5.
12. Let 2.3N HCL drip through. Throw away waste.
13. Change to white teflon beakers (250ml).
14. Change to 7.3N HCL.
15. Elute 150ml 7.3N HCL.
16. Place beakers on hot plate in clean air box at setting of 2.1 and let dry overnight.
17. Wash columns with 7.3N HCL (fill to top). After this elution columns are ready for backwashing.
18. Next day. Take beakers off hot plate and let dry.
19. Add 10ml REE blank solution (clean 7% HNO₃). Use 5ml Finnpiquette from Carr's lab.
20. Scrape residue with teflon stir rod and mix.
21. Pour into plastic bottles, label and cap.

The whole procedure takes approximately 8 hours from the time the furnace is turned on.

REFERENCES

- BVTP, 1981, Basaltic volcanism on the terrestrial planets: Lunar and Planetary Institute: New York, Pergamon Press, 1286 p.
- Bryan, W.B., Finger, L.W., and Chayes, F., 1969, Estimating proportions in petrographic mixing equations by least-squares approximation: *Science*, v. 163, p. 926-927.
- Carr, M.J., Feigenson, M.D., and Bennett, E.A., 1990, Incompatible element and isotopic evidence for tectonic control of source mixing and melt extraction along the Central American arc: *Contributions to Mineralogy and Petrology*, v. 105, p. 369-380.
- Carr, M.J., and Stoiber, R.E., 1990, Volcanism, in Dengo, G., and Case, J.E., eds., *The Caribbean region: Boulder, Colorado, Geological Society of America, The Geology of North America*, v. H, p. 375-391.
- Cervantes, J.F., and Soto, G.J., 1988, Sedimentacion y volcanismo tras-arco Plio-Cuaternarios en el area de Siquirres, Costa Rica: *Ciencia y Tecnologia*, v.12, p.19-26.
- Feigenson, M.D., and Carr, M.J., 1985, Determination of major, trace and rare-earth elements in rocks by DCP-AES: *Chemical Geology*, v. 51, p. 19-27.
- Feigenson, M.D., Hofmann, A.W., and Spera, F.J., 1983, Case studies on the origin of basalt II: The transition from tholeiitic to alkalic volcanism on Kohala volcano, Hawaii: *Contributions to Mineralogy and Petrology*, v. 84, p. 390-405.
- Hanson, G.N., 1980, Rare earth elements in petrogenetic studies of igneous systems: *Annual Reviews of Earth and Planetary Science*, v. 8, p. 371-406.
- Hofmann, A.W., and Feigenson, M.D., 1983, Case studies on the origin of basalt I: Theory and reassessment of Grenada basalts: *Contributions to Mineralogy and Petrology*, v. 84, p. 382-389.

- Irving, A.J., 1978, A review of experimental studies of crystal/liquid trace element partitioning: *Geochemica Cosmochimica Acta*, v. 42, p. 743-770.
- Kussmaul, S., 1987, Petrologia de las rocas intrusivas neogenas de Costa Rica: *Revista Geologica de America Central*, v. 7, p. 83-111.
- Minster, J-F., and Allegrè, C.J., 1978, Systematic use of trace elements in igneous processes. Part III: Inverse problem of batch partial melting in volcanic suites: *Contributions to Mineralogy and Petrology*, v. 68, p. 37-52.
- Molnar, P., and Sykes, L., 1969, Tectonics of the Caribbean and Middle America regions from focal mechanisms and seismicity: *Geological Society of America Bulletin*, v. 81, p. 1639-1684.
- Nicholls, I.A., and Harris, K.C., 1980, Experimental rare earth element partition coefficients for garnet, clinopyroxene and amphibole coexisting with andesitic and basaltic liquids: *Geochimica Cosmochimica Acta*, v. 44, p. 287-308.
- Reagan, M.K., and Gill, J.B., 1989, Coexisting calcalkaline and high-niobium basalts from Turrialba Volcano, Costa Rica: implications for residual titanates in arc magma sources: *Journal of Geophysical Research*, v. 94, p. 4619-4633.
- Schnetzler, C.C., and Philpotts, J.A., 1970, Partition coefficients of rare-earth elements between igneous matrix material and rock-forming mineral phenocrysts-II: *Geochimica Cosmochimica Acta*, v. 34, p. 331-340.
- Shimizu, N. and Kushiro, I., 1975, The partitioning of rare earth elements between garnet and liquid at high pressures: preliminary experiments: *Geophysical Research Letters*, v. 2, p. 413-416.
- Shaw, D.M., 1970, Trace element fractionation during anatexis: *Geochimica Cosmochimica Acta*, v. 34, p. 237-243.
- Tournon, J., 1973, Presence de basaltes alcalins recents au Costa Rica (Amerique Central): *Bulletin*, v. 63, p. 140-147, Paris.

- Tournon, J., 1984, Magmatismes du Mésozoïque à l'actuel en Amérique Centrale: l'exemple de Costa Rica, des ophiolites aux andésites: Doctoral Thesis, University of Pierre and Marie Curie, Paris, 335 p.
- Watson, S., and McKensie, D., 1990, Melt generation by plumes: a study of Hawaiian volcanism: EOS Transcripts, American Geophysical Union, v. 71, p. 1695.
- Weyl, R., 1980, Geology of Central America: Berlin, Gebrüder Borntraeger, 371 p.
- Wood, B.J., and Fraser, D.G., 1976, Elementary thermodynamics for geologists. London: Oxford University Press, 303 p.